

AD-A142 063

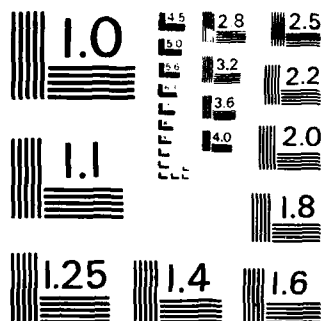
CERENKOV RADIATION GENERATED BY PERIODIC ELECTRON
BUNCHES IN A FINITE AIR PATH(U) NAVAL POSTGRADUATE
SCHOOL MONTEREY CA L A NEWTON DEC 83

1/1

UNCLASSIFIED

F/G 28/8

NL



MICROCOPY RESOLUTION TEST CHART
NATIONAL BUREAU OF STANDARDS - 1963 - A

(2)

NAVAL POSTGRADUATE SCHOOL

Monterey, California

AD-A142 063



DTIC
ELECTE
JUN 14 1984
S B

THESIS

DTIC FILE COPY

CERENKOV RADIATION GENERATED BY PERIODIC
ELECTRON BUNCHES IN A FINITE AIR PATH

by

Lawrence A. Newton

December 1983

Thesis Advisor:

F. R. Buskirk

Approved for public release; distribution unlimited

84 06 14 060

UNCLASSIFIED

SECURITY CLASSIFICATION OF THIS PAGE (When Data Entered)

REPORT DOCUMENTATION PAGE		READ INSTRUCTIONS BEFORE COMPLETING FORM
1. REPORT NUMBER	2. GOVT ACCESSION NO.	3. RECIPIENT'S CATALOG NUMBER
	AD A147 063	
4. TITLE (and Subtitle) Cerenkov Radiation Generated by Periodic Electron Bunches in a Finite Air Path		5. TYPE OF REPORT & PERIOD COVERED Master's Thesis December 1983
		6. PERFORMING ORG. REPORT NUMBER
7. AUTHOR(s) Lawrence A. Newton		8. CONTRACT OR GRANT NUMBER(s)
9. PERFORMING ORGANIZATION NAME AND ADDRESS Naval Postgraduate School Monterey, California 93943		10. PROGRAM ELEMENT, PROJECT, TASK AREA & WORK UNIT NUMBERS
11. CONTROLLING OFFICE NAME AND ADDRESS Naval Postgraduate School Monterey, California 93943		12. REPORT DATE December 1983
		13. NUMBER OF PAGES 62
14. MONITORING AGENCY NAME & ADDRESS (if different from Controlling Office)		15. SECURITY CLASS. (of this report) Unclassified
		15a. DECLASSIFICATION/DOWNGRADING SCHEDULE
16. DISTRIBUTION STATEMENT (of this Report) Approved for public release; distribution unlimited		
17. DISTRIBUTION STATEMENT (of the abstract entered in Block 20, if different from Report)		
18. SUPPLEMENTARY NOTES		
19. KEY WORDS (Continue on reverse side if necessary and identify by block number) Cerenkov radiation electron beams		
20. ABSTRACT (Continue on reverse side if necessary and identify by block number) Microwave Cerenkov radiation is measured for the case of bunched electron beams which exceed the velocity of light in a finite air path. The theoretical equation for prediction of the form of the power for Cerenkov radiation is tested experimentally for this case. Initial verification of the theory is observed.		

DD FORM 1 JAN 73 1473

EDITION OF 1 NOV 65 IS OBSOLETE
S/N 0102- LF-014-6601

UNCLASSIFIED

SECURITY CLASSIFICATION OF THIS PAGE (When Data Entered)

Approved for public release; distribution unlimited.

Cerenkov Radiation Generated
by Periodic Electron Bunches
in a Finite Air Path

by

Lawrence A. Newton
Lieutenant, United States Navy
B.A., University of California, San Diego, 1974
M.B.A., San Diego State University, 1978

Submitted in partial fulfillment of the
requirements for the degree of

MASTER OF SCIENCE IN PHYSICS

from the

NAVAL POSTGRADUATE SCHOOL
December 1983

Author:

Lawrence A. Newton

Approved by:

Fred R. Burkhill

Thesis Advisor

John R. Neighbors

Second Reader

G. E. Schacher

Chairman, Department of Physics

Wm. Dyer

Dean of Science and Engineering

ABSTRACT

Microwave Cerenkov radiation is measured for the case of bunched electron beams which exceed the velocity of light in a finite air path. The theoretical equation for prediction of the form of the power for Cerenkov radiation is tested experimentally for this case. Initial verification of the theory is observed.

Accession For	
NTIS GRA&I	<input checked="checked" type="checkbox"/>
DTIC TAB	<input type="checkbox"/>
Unannounced	<input type="checkbox"/>
Justification	
By	
Distribution/	
Availability Codes	
Dist	Avail and/or Special
A-1	



TABLE OF CONTENTS

I.	INTRODUCTION	7
II.	EXPERIMENT	14
	A. BASIC EXPERIMENTAL DESIGN	14
	B. EXPERIMENTAL APPARATUS	15
	1. LINAC	16
	2. Air Path	16
	3. Mirror	17
	4. End Station Detection Apparatus	17
	5. Cable	21
	6. Observer Station	21
III.	RESULTS	25
	A. METHOD OF DATA REDUCTION	25
	B. DATA	25
	C. CONCLUSIONS	32
APPENDIX A: FORTRAN PROGRAM FOR CALCULATING CERENKOV RADIATION CURVES		35
APPENDIX B: FORTRAN PROGRAM - CERENKOV CURVES WITH DATA POINTS		40
APPENDIX C: FORTRAN PROGRAM - SUM OF CERENKOV CURVES WITH DATA POINTS		46
APPENDIX D: EXPERIMENTAL APPARATUS		52
APPENDIX E: TABULAR DATA FOR FIGURES		56
LIST OF REFERENCES		61
INITIAL DISTRIBUTION LIST		62

LIST OF TABLES

I.	Variable Definitions	10
II.	LINAC Parameters	16
III.	Tabular Data for Figure 3.1	56
IV.	Tabular Data for Figure 3.2	57
V.	Tabular Data for Figure 3.3	58
VI.	Tabular Data for Figure 3.4	59
VII.	Tabular Data for Figure 3.5	60

LIST OF FIGURES

1.1	Cerenkov Radiation	8
1.2	Third Harmonic for $L = 0.7, 0.9, 1.5$ meters . . .	12
1.3	Harmonics 3,5,7 for $L = 1.0$ meters	13
2.1	Experimental Design	15
2.2	Antenna Beam Profile for the Electric Field . .	19
2.3	Antenna Beam Profile for the Magnetic Field . .	20
2.4	Filter Band-pass for the Third Harmonic	22
2.5	Filter Bandpass for the Fourth Harmonic	23
3.1	Harmonic=3 : $L=1.0$ m: Filter = 3rd	27
3.2	Harmonic=4 : $L = 1.0$ m : Filter=4th	28
3.3	Harmonics= 3-7 : $L = 1.0$ m : Filter = Waveguide	29
3.4	Harmonics= 3 + 4 : $L=1.0$ m : Filter = Waveguide	32
3.5	Harmonics= 3 + 6 : $L=1.0$ m : Filter = 3rd . . .	33
D.1	LINAC End-Station	53
D.2	Detection Apparatus Components	54
D.3	Assembled Detection Apparatus	55

I. INTRODUCTION

Since the speed of light is modified by the index of refraction in a dielectric, it is possible for relativistic electrons to have a velocity which actually exceeds that of light in the medium. In this circumstance a phenomenon known as Cerenkov radiation arises. This radiation appears in a cone, around the direction of motion of the electrons, defined by the Cerenkov angle.

$$\theta_c = \cos^{-1} (c/nv), \quad (\text{eqn 1.1})$$

where c is the speed of light in a vacuum, n is the index of refraction, and v is the velocity of the electrons. This radiation is analogous to acoustic shock waves in air.

F. R. Buskirk and J. R. Neighbours [Ref. 1] calculated the power of Cerenkov radiation for the case where the electrons are bunched and the dielectric medium is of finite length. The experiments described in this thesis were designed to check those theoretical calculations.

Figure 1.1 depicts the pertinent physical relationships for this situation. See Table I for definitions of the variables. The first step in the theoretical derivation was to calculate the vector potential \underline{A} and the scalar potential, ϕ , at a field point \underline{r} resulting from an element of charge at a location within the electron bunch. A key factor in the analysis is that the current and charge densities which appear in the expressions for the potentials are periodic and may be expressed as Fourier series. Therefore, the potentials themselves may also be expressed as Fourier series, with Fourier coefficients representing the frequency components.

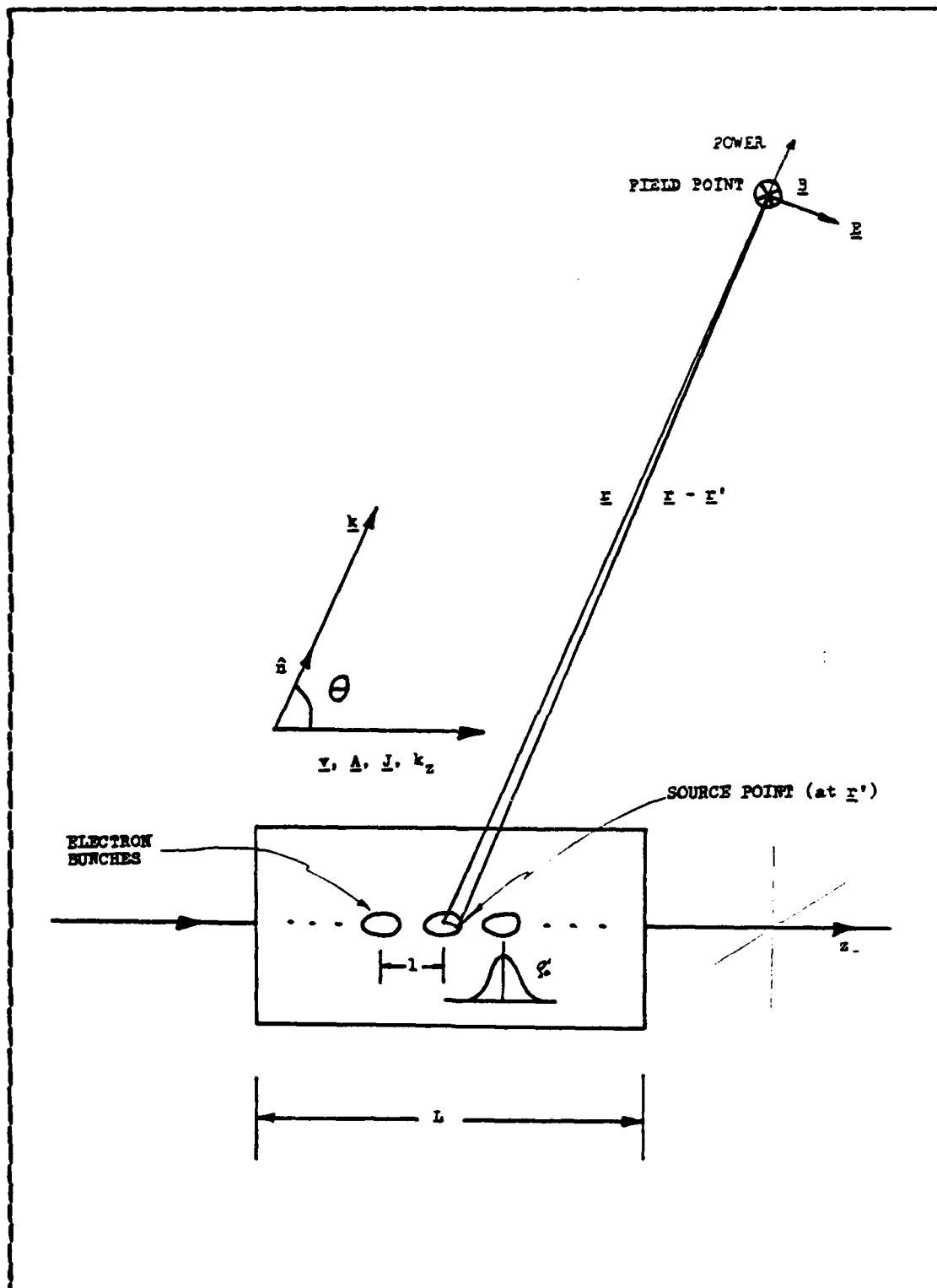


Figure 1.1 Cerenkov Radiation.

It is convenient to carry out the rest of the analysis in terms of the Fourier coefficients. The electric and magnetic field components are obtained from the potentials, and these, in turn, are used to find the frequency components of the average radiated power. An important assumption inherent in the procedure, which may directly affect experimental validity, is that the field point is assumed to be far from the source region. For details of the entire analysis, see [Ref. 2].

A principal result of [Ref. 2] is slightly recast in [Ref. 3] as the following expression for the power per unit solid angle at a given frequency,

$$W(\nu, n) = \frac{\mu}{2c} L^2 \nu^2 \nu_0^2 \sin^2 \theta |\rho'_0(\underline{k})|^2 I^2(u) , \quad (\text{eqn 1.2})$$

with the parameters defined as follows:

$$u = \frac{kL}{2} (\cos \theta_c - \cos \theta) , \quad (\text{eqn 1.3})$$

$$I(u) = \frac{\sin u}{u} , \quad (\text{eqn 1.4})$$

and

$$\rho'_0(\underline{k}) = \iiint_{-\infty}^{\infty} d^3 r e^{-i \underline{k} \cdot \underline{r}} \rho'_0(\underline{k}) . \quad (\text{eqn 1.5})$$

Refer to figure 1.1 and table I for clarification of these parameters.

The frequencies appearing in equation 1.2 are harmonics of the electron bunch frequency, which is a constant (ν_0). Thus, writing (ν) as ($j \nu_0$), and using a one-dimensional

TABLE I
Variable Definitions

\underline{J}	= $\rho \underline{v}$	= current density
l	= \underline{v}/ν_0	= bunch spacing
ν_0	=	bunch frequency
\underline{v}	=	bunch velocity
\underline{k}	=	power propagation direction
\underline{n}	=	unit vector in the \underline{k} direction
L	=	length of finite emission region
\underline{A}	=	vector potential
\underline{r}	=	position vector of field point
\underline{r}'	=	position vector of source point
ρ'	=	Gaussian distribution of longitudinal bunch (charge) distribution
b	=	parameter for the charge distribution
\underline{E}	=	electric field vector
\underline{B}	=	magnetic field vector

Gaussian distribution to describe the longitudinal bunch dimension, a relatively simple Cerenkov radiation power function is given by equation 1.6 (equations 9 and 10 of [Ref. 3]). This is the expression which was used to compare theoretical to experimental results.

$$P_j(\theta) = \frac{2\mu\nu_0^4 q^2}{c} \frac{1}{4} L^2 \sin^2 \theta \left(\frac{\sin u}{u} \right)^2 \text{Exp} \left(\frac{-k_z^2 b^2}{2} \right), (\text{eqn 1.6})$$

Note that the radiation function varies with the square of the harmonic number, the length L of the emission region, and the angle at which the radiation is being observed. Note also the interference factor, similar to what might be experienced with optical radiation, and the way in which the bunch dimension, b , appears in the expression. The length of the emission region and the angle appear not only directly, but also through the factor u (see equation 1.3).

The results of this simple equation are quite interesting. Due to the finite size of the emission region, radiation no longer appears only at the Cerenkov angle, but throughout a range of angles determined by the $(\sin u)/u$ factor. Figure 1.2 shows how the radiation is spread for three different sizes of emission region. For a given harmonic, smaller emission regions cause greater spread, or diffraction of the radiation. The power is distributed to varying degrees among the different harmonics also, as depicted by figure 1.3. Higher harmonics have larger peak powers, and are peaked at a smaller angle than are lower harmonics.

For this experiment, the microwave portion of the spectrum was investigated, and the dielectric medium for the electron path was chosen to be air. The electrons were accelerated to relativistic velocities by the Naval Postgraduate School LINAC, which produces electrons with energies of approximately 100 Mev. For the theoretical calculations, a Fortran program (see appendix A) was used to calculate the power as a function of angle from equation 1.6. Variants of this program (appendices B and C) were used to superimpose data points over the theoretical curves.

The experimental apparatus and procedures are described in detail in the next chapter.

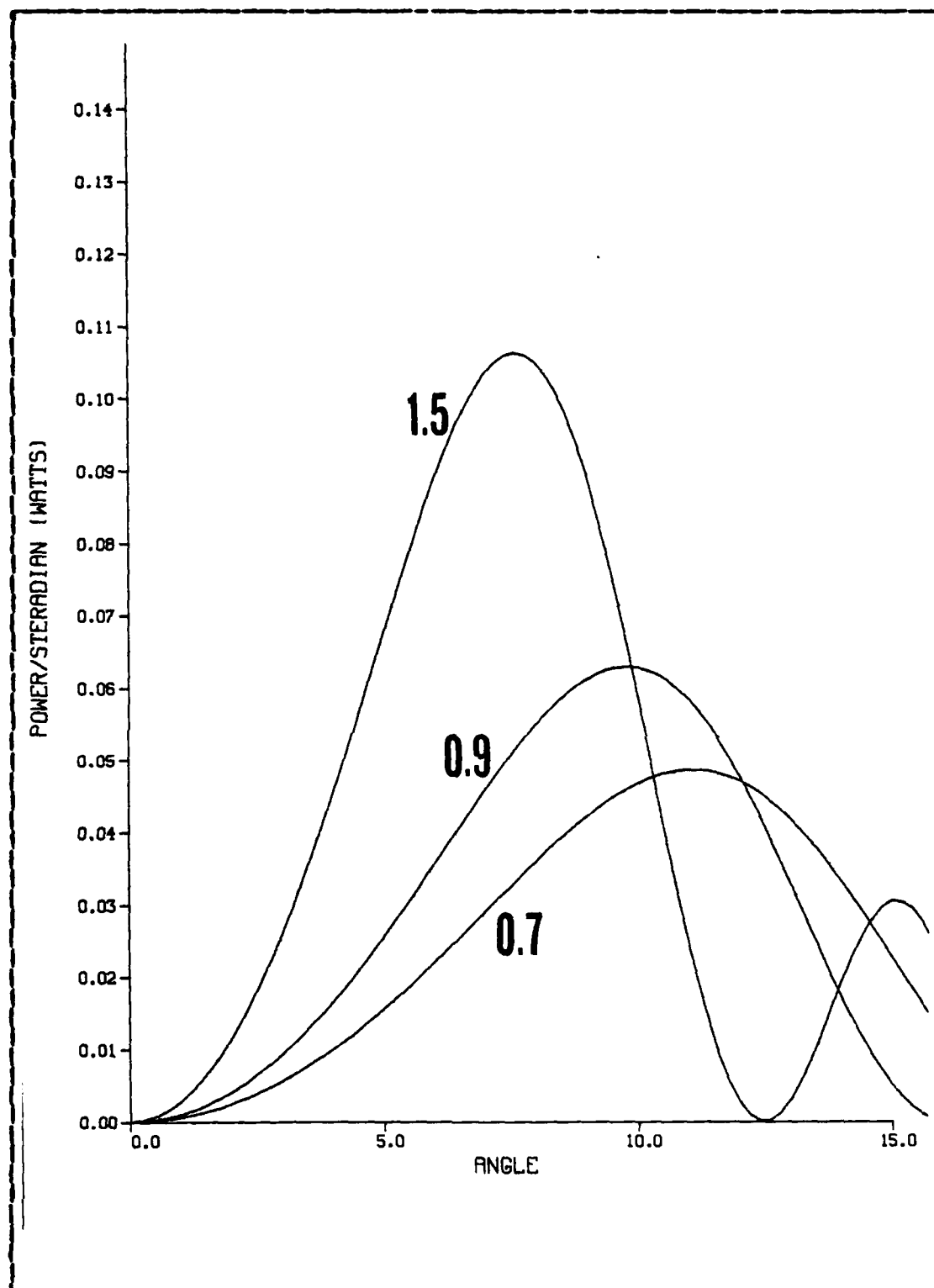


Figure 1.2 Third Harmonic for $L = 0.7, 0.9, 1.5$ meters.

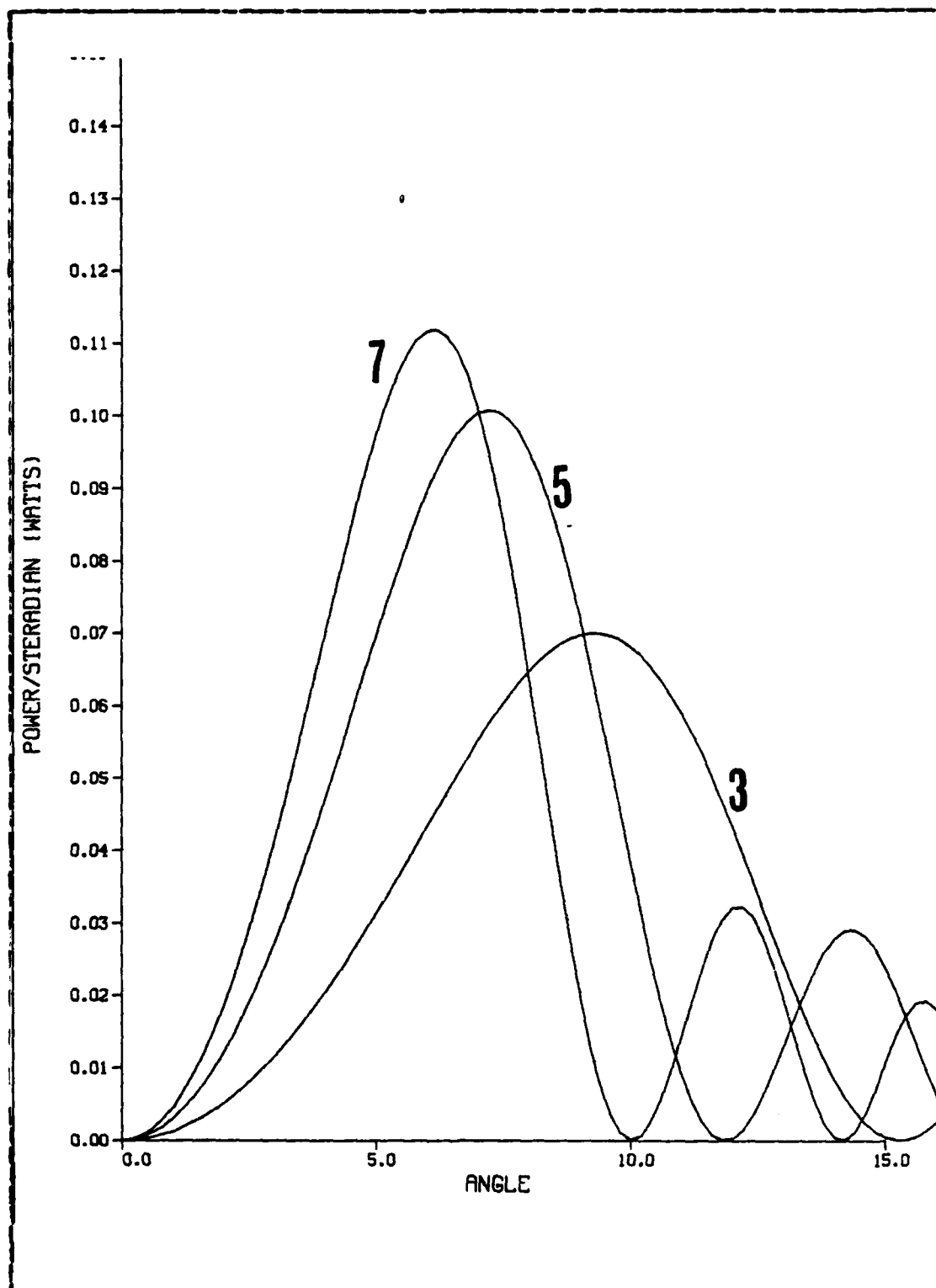


Figure 1.3 Harmonics 3,5,7 for $L = 1.0$ meters.

II. EXPERIMENT

A. BASIC EXPERIMENTAL DESIGN

The purpose of this experiment was to measure the power from Cerenkov radiation as a function of angle, in order to compare it with theoretical curves such as those depicted in figures 1.2 and 1.3. The basic design for this experiment is shown in figure 2.1. Photographs of the experimental apparatus are presented in Appendix D. The electron bunches exit the Linac aperture and emit Cerenkov radiation until they reach the aluminum mirror. This mirror allows the electrons to pass and proceed into the beam dump, while the microwave radiation of interest is reflected into the detector area. The mirror therefore performs the function, required by theory, that the radiation be emitted over a finite distance. The detector is mounted on a pivot arm, which is placed such that the detector is always pointed at the virtual center of the emission region. The pivot arm also fixes the distance from the center of the emission region to the detector, so that the distance over which the radiation travels is eliminated as a variable.

With this experimental setup, the basic experimental procedure was to sweep the detector over the angular range of interest using a small motor in the detector mount. The signal picked up by the detector was transmitted to the observer station, where it was fed into an amplifier and then into both an oscilloscope and a pulse height analyzer. The oscilloscope allowed a gross measure of power, while the frequency distribution measured by the pulse height analyzer gave a more precise value. The end result of this procedure was tabular data in the form of signal versus angle.

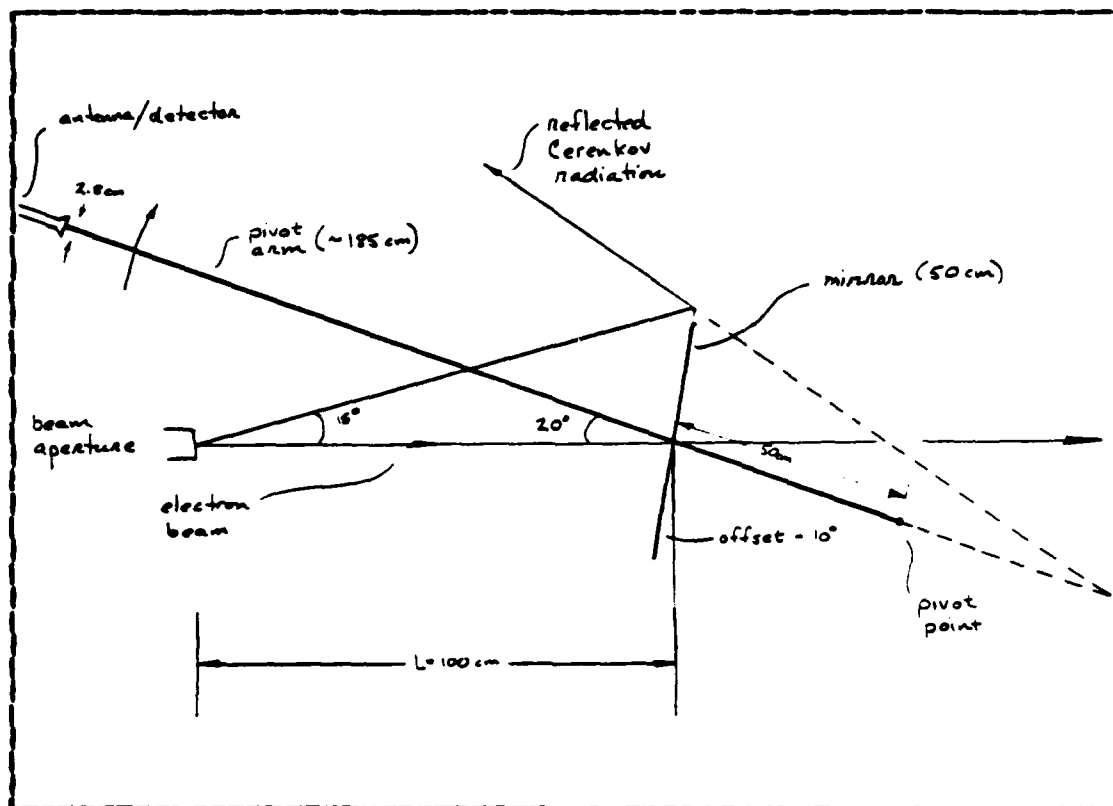


Figure 2.1 Experimental Design.

This brief overview of the experimental design is amplified in the next section with a more detailed look at various elements of the experimental apparatus.

B. EXPERIMENTAL APPARATUS

In this section, the components of the experimental apparatus will be examined, in order to provide a precise understanding of the experiment. The various components of the signal train will be reviewed in order, from the originating device (LINAC) to the final detection and analysis components.

1. LINAC

The salient features of the LINAC are listed in table II. These parameters are the same as those calculated by A. Saglaa in prior thesis work with the LINAC at the

TABLE II
LINAC Parameters

Bunch Frequency:	2.856 GHz
Bunch Velocity:	$2.997886E08$ m/s
Bunch Size Parameter:	0.24 cm
Electron Energy:	100 MeV
Bunch Spacing:	10.5 cm

Naval Postgraduate School [Ref. 4]. These parameters also meet those chosen in [Ref. 3] which gives the theoretical curves for Cerenkov radiation. The LINAC provided fairly consistent signals for the experiments which are reported here. However, the signal eventually developed instabilities which precluded further experiments. That is, it became impossible to distinguish between signal variation due to the LINAC and that due to variation in the angle of detection. It may be that some of the experimental deviation from theory can be adequately explained by the variability of the LINAC itself.

2. Air Path

The air path was chosen to be 1.0 meter in length, which was convenient for the dimensions of the LINAC end station. The characteristic index of refraction for air was taken to be 1.000268, which is the same as that given for

air in [Ref. 3]. This gives a speed of light in air of 2.997127E08 meters per second, which is less than the velocity of 100 Mev electrons (see Table II).

3. Mirror

A polished aluminum mirror 50 centimeters in length was used to fix the path length. The mirror performed the dual function of allowing the electron bunches to pass and proceed into the beam dump, while causing the microwave Cerenkov radiation to be reflected into the detection area. The electron bunches continued to emit Cerenkov radiation after passing through the mirror. It was assumed that this radiation did not reach the detection area, due to the inherent weakness of the signal, and due to the distance and multiple reflections it would have to travel through in order to reach the detection area.

The mirror was tilted 10 degrees, causing the reflection axis to be offset 20 degrees from the beam axis. Therefore, the actual length of the emission region varied between approximately 95 and 105 centimeters. Measurements were made over a range of from 0 to 15 degrees. The mirror was long enough to reflect most, but not all, of the radiation at 15 degrees. See figure 2.1 for details of the geometry of the experiment.

4. End Station Detection Apparatus

The detection apparatus was mounted at the end of a pivot arm of fixed length. The pivot point was located at the center of the virtual image projected by the mirror, in order for the detector to always be pointed at the virtual center of the emission region. Theory assumed that the emission region would be a short distance, small compared to the detector distance z' (field point). Focusing the detector on the center of the emission region was done to

approximate theory as closely as possible. The pivot arm also kept the detector at a fixed distance from the (virtual) center of the emission region. Therefore, the distance of travel of the measured radiation was approximately the same for all angles, so that variation in distance would have minimal effect on the signal variation.

a. Antenna

A small antenna, with a lateral dimension of 2.8 centimeters, served as the forward end of the detection apparatus. This antenna served two functions. First, it was small enough that, with the given length of the pivot arm, the antenna subtended an arc length of approximately 1 degree. Therefore, an experimental measurement resolution of 1 degree was obtained. Further, this antenna had a very wide beam width. The antenna profiles for the electric and magnetic fields are given in figures 2.2 and 2.3. Using the half-power points as cutoffs, the beam width is found to be greater than 60 degrees for both the E and H fields, and thus for the power as well. At a distance equal to the average of that between the antenna and the mirror, approximately 130 centimeters, the beamwidth covers an arc length of 68 centimeters, which is larger than the length of the mirror.

Therefore, radiation arriving at the antenna and originating from any part of the emission region would be collected by the antenna. This again approximates the theoretical condition that the emission region be a point source, since the antenna "sees" the entire emission region at every angle of interest.

In summary, the antenna's narrow dimensions have provided spatial resolution, while its wide beamwidth has approximated a theoretical requirement.

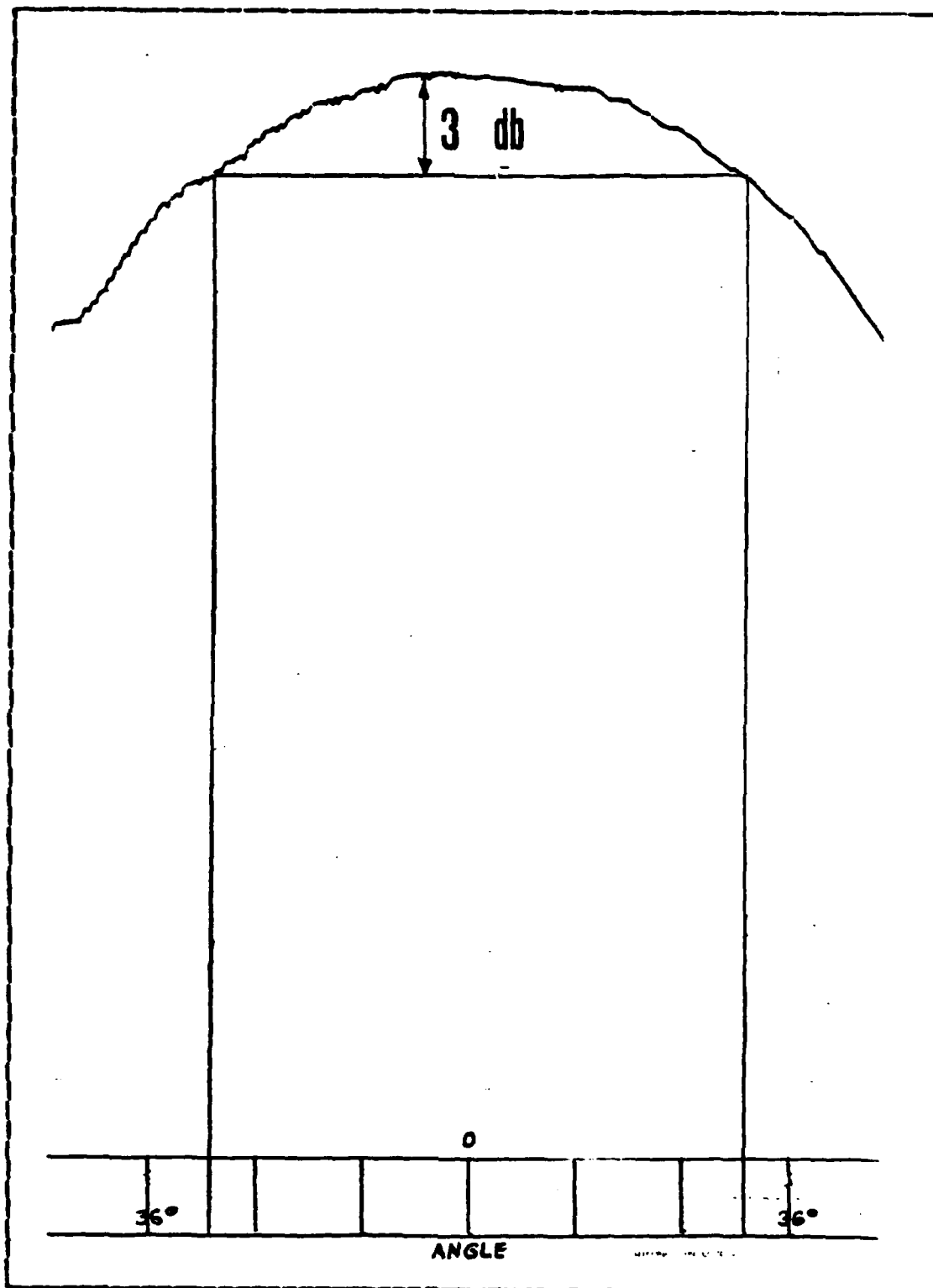


Figure 2.2 Antenna Beam Profile for the Electric Field.

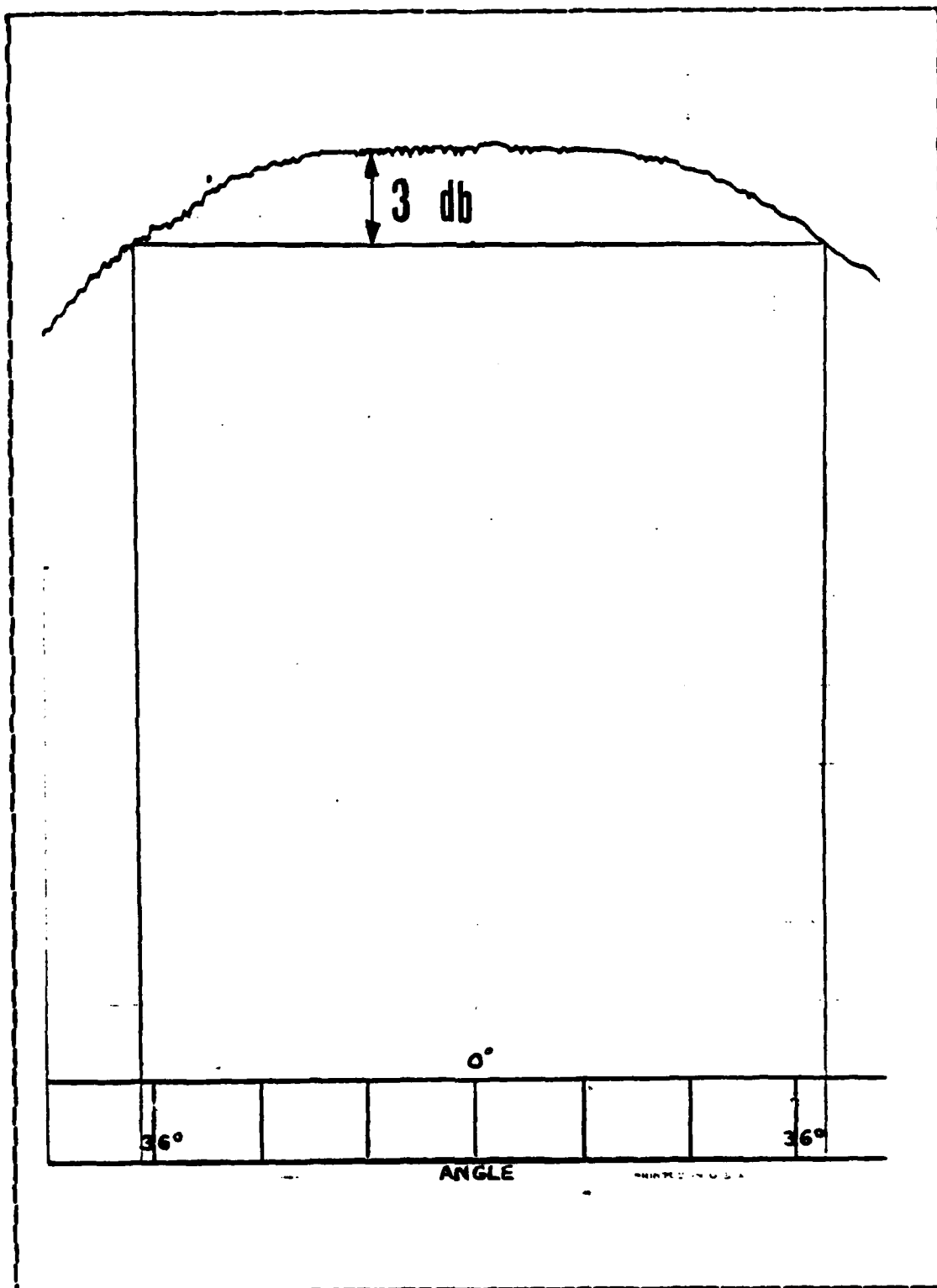


Figure 2.3 Antenna Beam Profile for the Magnetic Field.

b. Filters

In previous experiments reported in [Ref. 4] a section of X-band waveguide was included between the antenna and the crystal detector. This waveguide serves as a partial filter of the microwave radiation, since it does not pass the fundamental frequency (2.86 GHz) nor the second harmonic (5.71 GHz). Use of the X-band waveguide as a filter was included as one of the variants in this experiment. Additionally, filters were available which were able to select the third and the fourth harmonics of the bunch frequency. These filters were designed and built by K. Alexander and S. Hamel [Ref. 5]. The band-pass characteristics for these filters are shown in figures 2.4 and 2.5.

c. Detector

The final component in the detection apparatus was the detector itself, an HP X-band X424A crystal detector. The detector was used without the square-law load. Therefore, the response varied linearly with the input (Cerenkov) signal.

5. Cable

In the work done by A. Saglam [Ref. 4] the experimental area (end station of the LINAC) was described as very noisy due to the electromagnetic energy radiated by the LINAC klystrons. This problem was effectively solved in this experiment by using doubly-shielded cable to transmit the detected signal to the observer station.

6. Observer Station

The analyzing equipment consisted of an ORTEC 450 Research Amplifier, a TEKTRONIX 7904A Oscilloscope, and a TRACER NORTHERN TN-7200 Pulse Height Analyzer (PHA). The

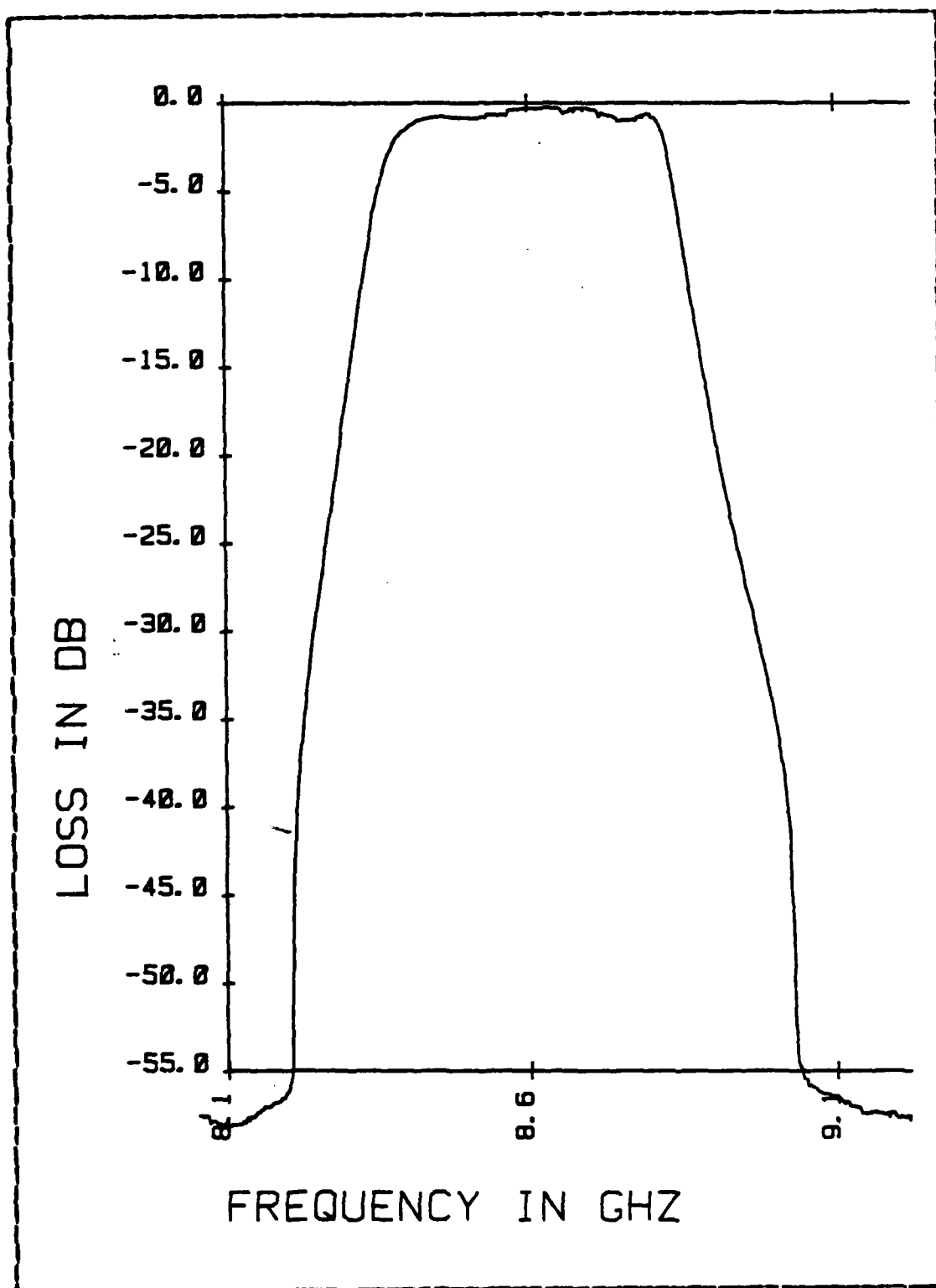


Figure 2.4 Filter Band-pass for the Third Harmonic.

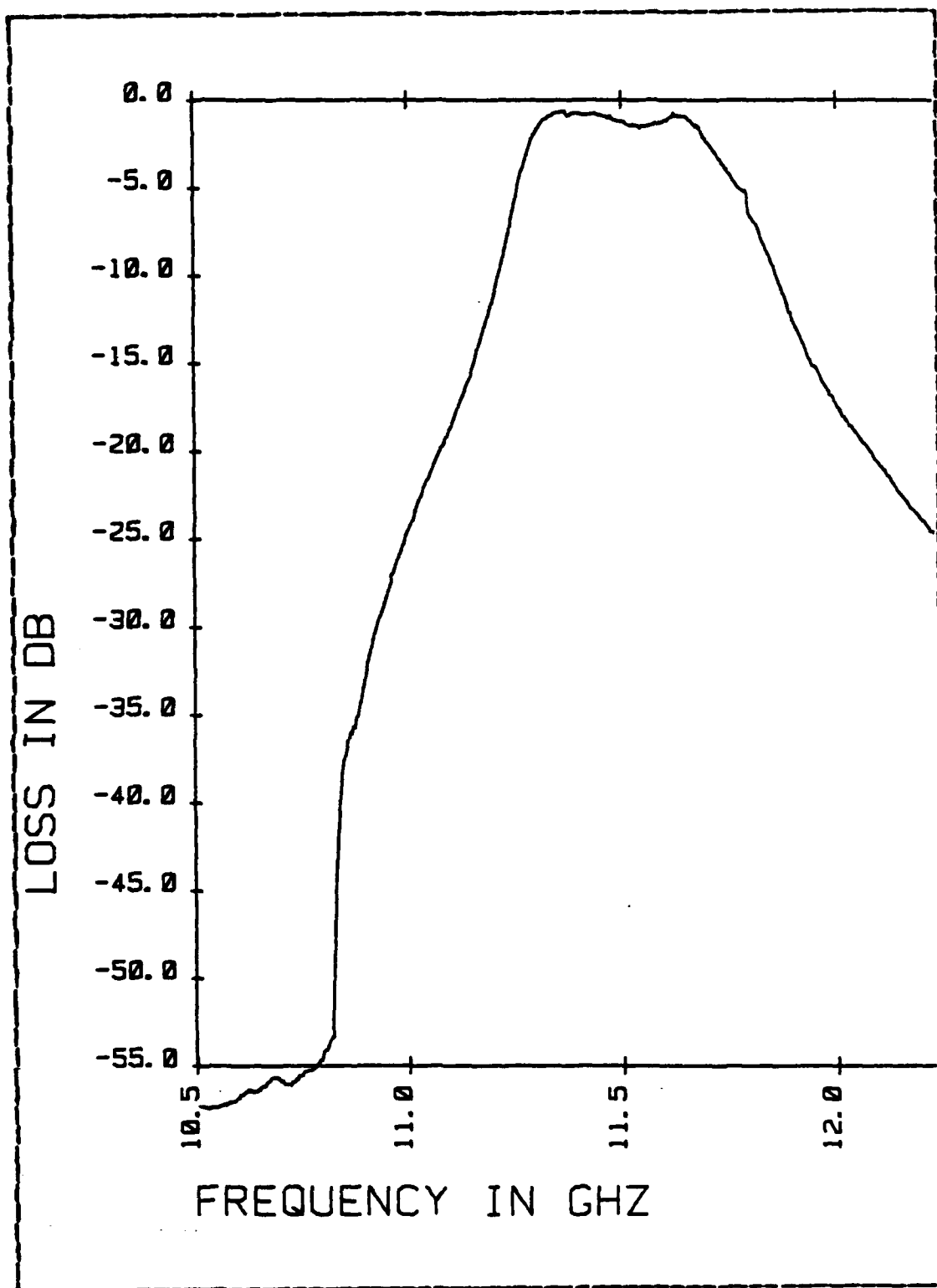


Figure 2.5 Filter Bandpass for the Fourth Harmonic.

critical piece of equipment for experimental purposes was the PHA. This instrument divided the detection range into a predetermined number of channels (e.g. 1024) and then recorded graphically the frequency with which each signal channel was detected. This allowed the observer to deal with a certain degree of variability in the signal, by choosing the observed value to be the peak of the frequency distribution. The frequency distributions observed ranged from very sharp spikes at the lower signal levels to typically broader peaks at higher signal levels. The PHA display also provided an measure of LINAC stability. If the frequency distribution of the detected signal was extremely broad or if multiple peaks were formed while detection angle remained constant, machine instabilities were indicated.

This concludes the discussion of the experimental apparatus. Comparison of experimental results to theoretical curves is presented in the next chapter.

III. RESULTS

A. METHOD OF DATA REDUCTION

As explained in Chapter 2, the raw data from the experiment was in the form of signal (power) versus angle. Since the signal was processed through a series of elements (filter, detector, amplifier, PHA), a measurement of the absolute power was not available. Therefore, it was necessary to normalize these measurements in order to make comparisons with the theoretical curves. The method of normalization chosen was the matching of peaks. For a given experiment, the experimental points were examined to determine which one had the peak value. This value was then adjusted such that it exactly matched (in magnitude) the peak value of the appropriate theoretical curve. All other experimental points for that experiment were then adjusted by the same factor, so that the experimental points maintained the same relative magnitudes.

B. DATA

The results presented here are characteristic for the experiments which were performed. Each figure shows the theoretical curve for the harmonics assumed to be present for a given filter, with the experimental points overlaid and normalized to the peak value of the theoretical curve. Tabular data for figures 3.1 through 3.5 are presented in Appendix E. Figure 3.1 and 3.2 compare the theoretical curves for harmonics three and four to the radiation measured with the appropriate filters inserted before the detector. Figure 3.3 compares the theoretical curve for the sum of harmonics three through seven with the radiation

measured with an X-band waveguide inserted before the detector.

These results appear to be good enough to indicate an initial verification of the theory. Results were best for the fourth harmonic (figure 3.2), with very close agreement between theory and experimental points. The experimental results for the third harmonic (figure 3.1) are shifted somewhat to the left of theory, while the results for the sum of harmonics (figure 3.3) are shifted to the right.

One predicted effect which is clearly evident despite the shifting is the relative spread of the Cerenkov angle for different harmonics. The third harmonic is predicted to spread the radiation over a broader range of angles than does the fourth harmonic, and this is verified by the experimental results.

There are several possible explanations for the deviations from theory which are shown here. For example, certain assumptions necessary for theoretical simplicity may not hold in the experimental situation. It may be that the charge distribution of the electron bunches is not Gaussian, or that a lateral parameter should be included in the Gaussian to account for divergence of the beam over the air path. Another factor possibly affecting the results was the mirror tilt, which caused the air path length to be longer than one meter on one side of the beam, and shorter on the other.

Another factor which must affect the results to some degree is simply the experimental geometry. For a number of reasons, theory calls for the field point distances to be much greater than the source point distances. That is, the path length should be small in relation to the distance to the point at which the fields are measured. However, the dimensions of the LINAC end station prohibit this, so that at angles larger than just a few degrees, there is ambiguity

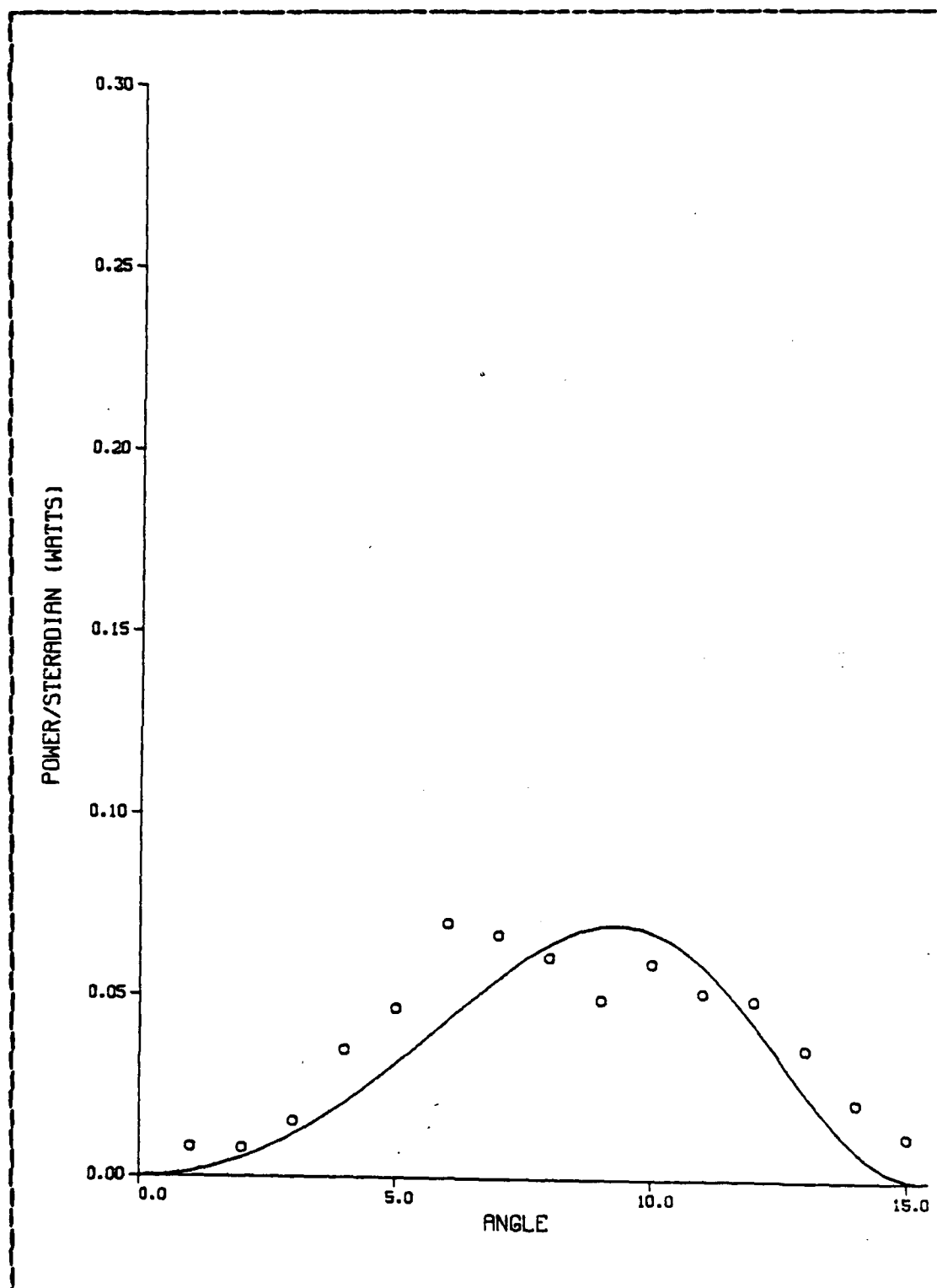


Figure 3.1 Harmonic=3 : L=1.0 m: Filter = 3rd.

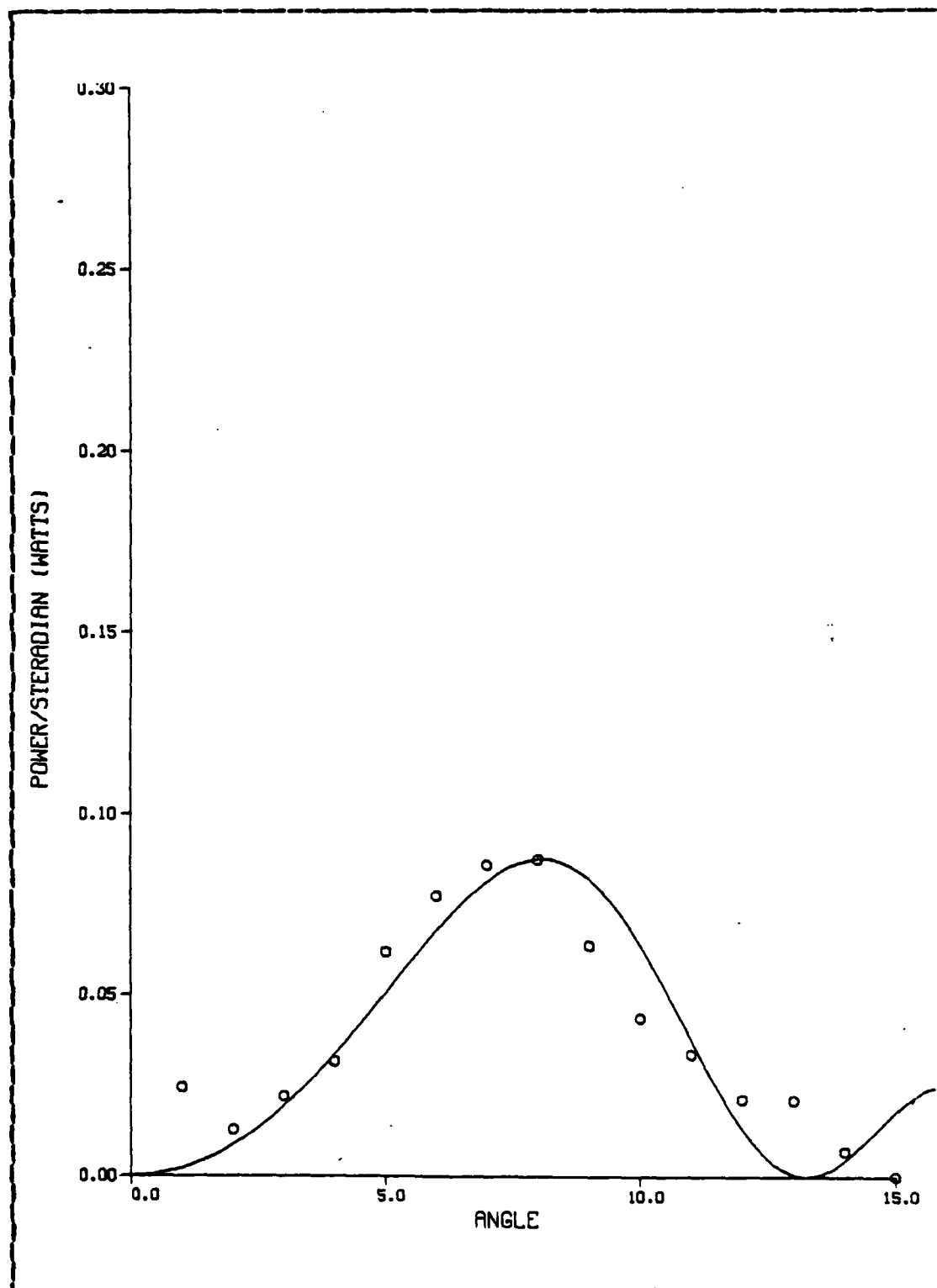


Figure 3.2 Harmonic=4 : L = 1.0 m : Filter=4th.

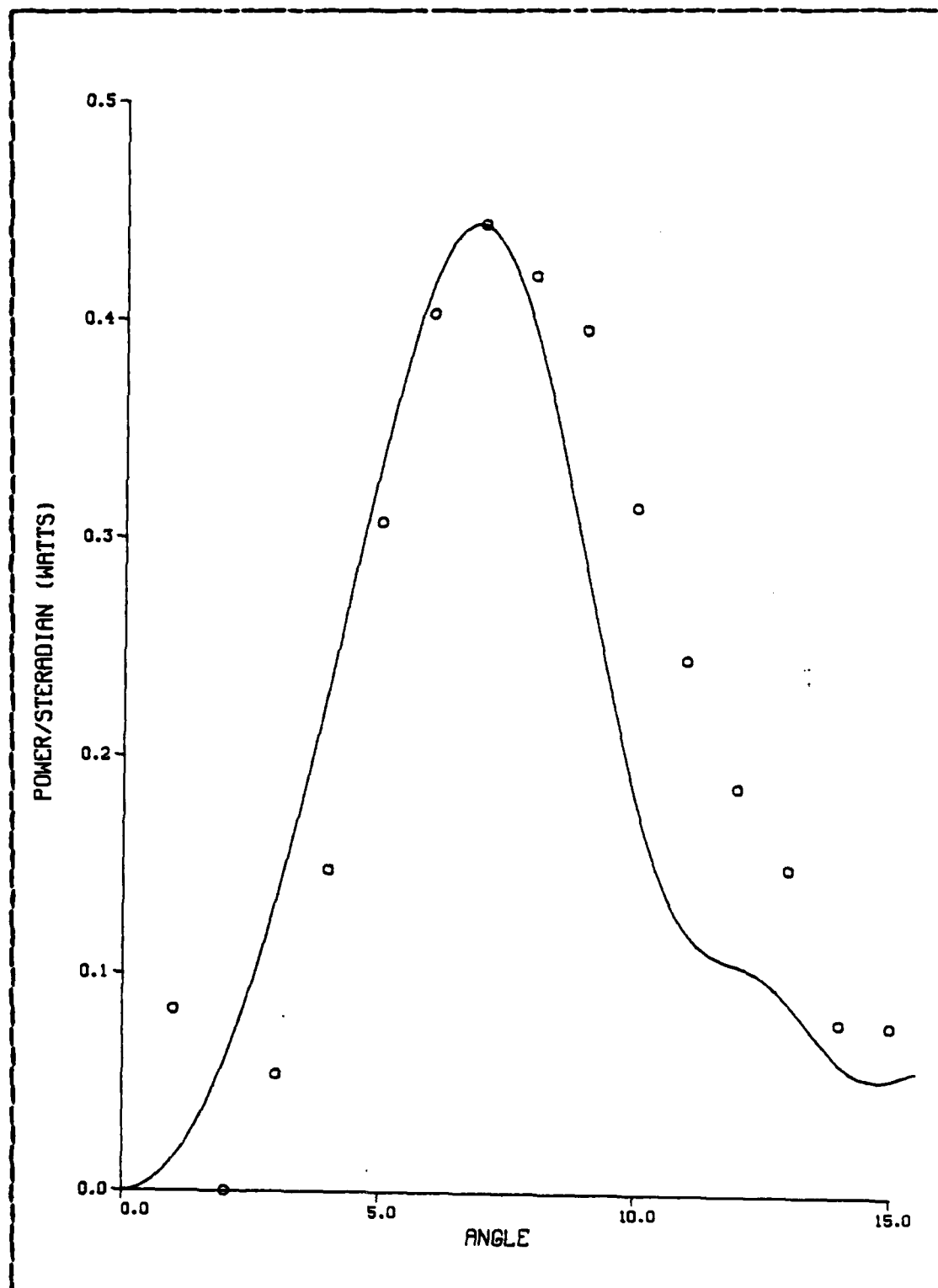


Figure 3.3 Harmonics= 3-7 : $L = 1.0 \text{ m}$: Filter = Waveguide.

regarding exactly which angle is being measured. For small observation angles, the air path does look like a point, but as the angles become larger there are increasing differences between the angle as measured from the beginning of the air path and the angle as measured from the end of the air path. At large angles (greater than five degrees) the angle as measured from the center of the air path is substantially smaller than that measured from the end of the path. Since the radiation originating from the end of the path is stronger (it has traveled a smaller distance to the detector), and since this radiation originates at an angle larger than that which is being measured, the radiation at the measured angle is actually overstated. This may be the cause of the shift to higher angles observed in figure 3.3.

Finally, the frequency range over which the filters are valid must be considered. The X-band filters and waveguide used in this experiment are designed for use with radiation in the frequency range 8.2 to 12.4 GHz. Radiation within this band will only propagate in the dominant TE mode in X-band waveguide. Note that this encompasses only the third (8.57 GHz) and the fourth (11.42 GHz) harmonics of the LINAC bunch frequency. When radiation outside this frequency band is fed into the waveguide (as with the fifth and higher harmonics of the bunch frequency which are expected in Cerenkov radiation), modes other than the dominant may be excited in the waveguide. As indicated by [Ref. 6], the effects of coupling multiple modes into and out of a waveguide are complex, and the normal single probe configuration for detecting signal energy in the dominant mode cannot be reliably used in this situation. Since frequencies outside the X-band operating range were expected to be present in this experiment, modes higher than the dominant may have been excited, thereby causing inaccuracies in the measurement of power by the signal detector.

A comparison was made to test for the possibility that frequencies outside the X-band operating range were not being accurately measured by the single probe detector. Figure 3.3 compares the theoretical sum of harmonics 3-7 with the data measurements from the X-band waveguide, using no filter in the waveguide. Adding higher harmonics to the sum, although theoretically correct, would cause a larger discrepancy between theory and experiment, since higher harmonics are shifted towards smaller angles. Assuming the worst case, that harmonics five and above excite modes in the waveguide which are somehow not correctly coupled and detected, implies the possibility that only harmonics three and four are being measured when X-band waveguide is used as a filter. Figure 3.4, showing the data gathered with the waveguide filter normalized against the sum of harmonics three and four, appears to fit the data better, in that the width of the theoretical curve is more closely approximated by the experimental points than in figure 3.3. This lends some credence to the supposition that the detector does not respond well to harmonics higher than the fourth.

A second comparison was made to investigate the possibility that the filters which were used to isolate the third and fourth harmonics were also passing higher resonant frequencies. Such higher frequencies would be close to multiples of the frequency which the filter was designed to pass. For example, figure 3.1 compares the data gathered with the filter for the third harmonic to the theoretical curve for the third harmonic. Figure 3.5 compares the same data to the theoretical sum of the third and sixth harmonics. Note that a somewhat better fit of the data at the smaller angles is obtained in figure 3.5, indicating that the filter may be passing higher resonant frequencies, which in this case are measured by the detector, despite the effects of higher modes which may have been excited.

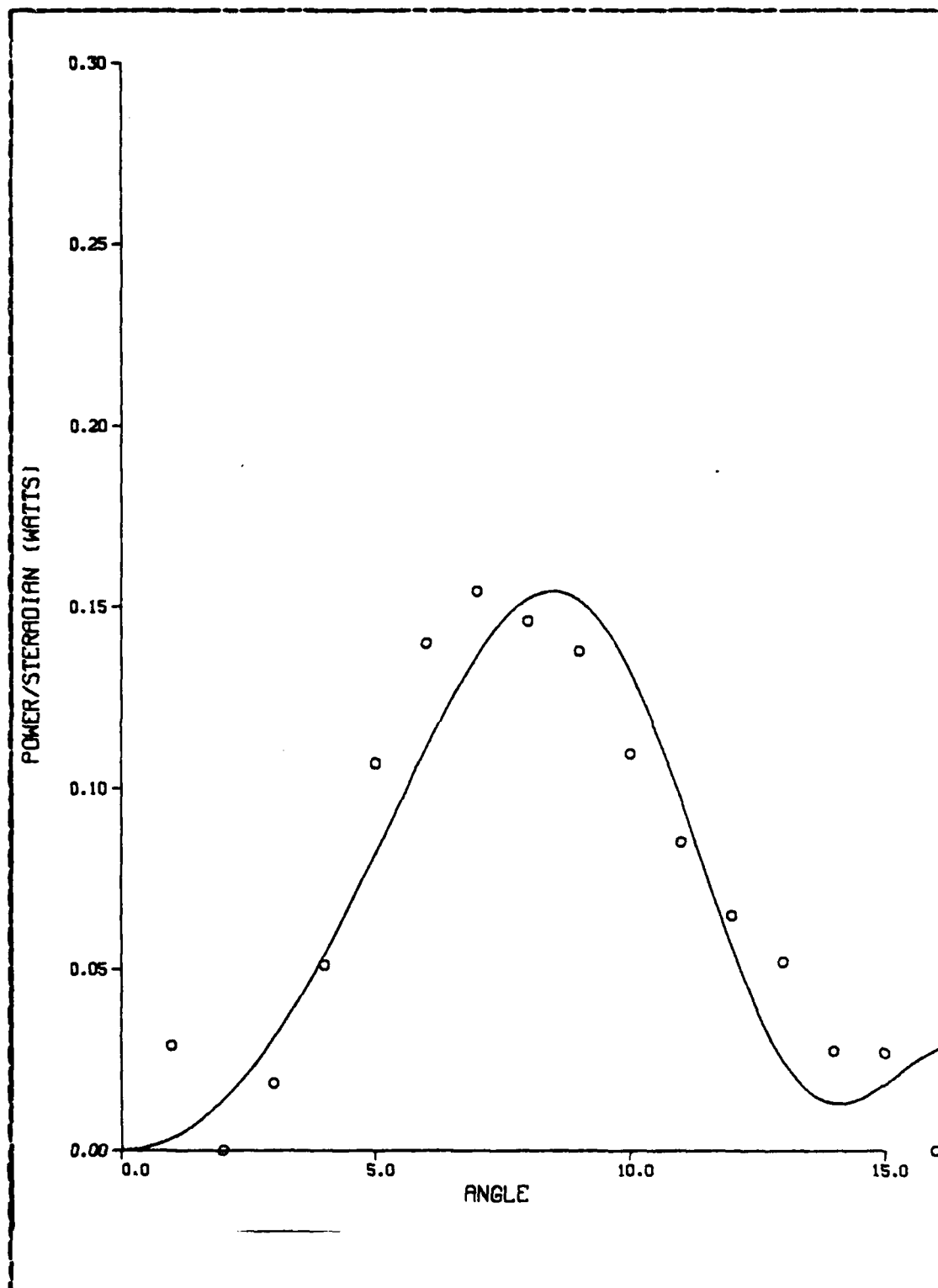


Figure 3.4 Harmonics= 3 + 4 : L=1.0 m : Filter = Waveguide.

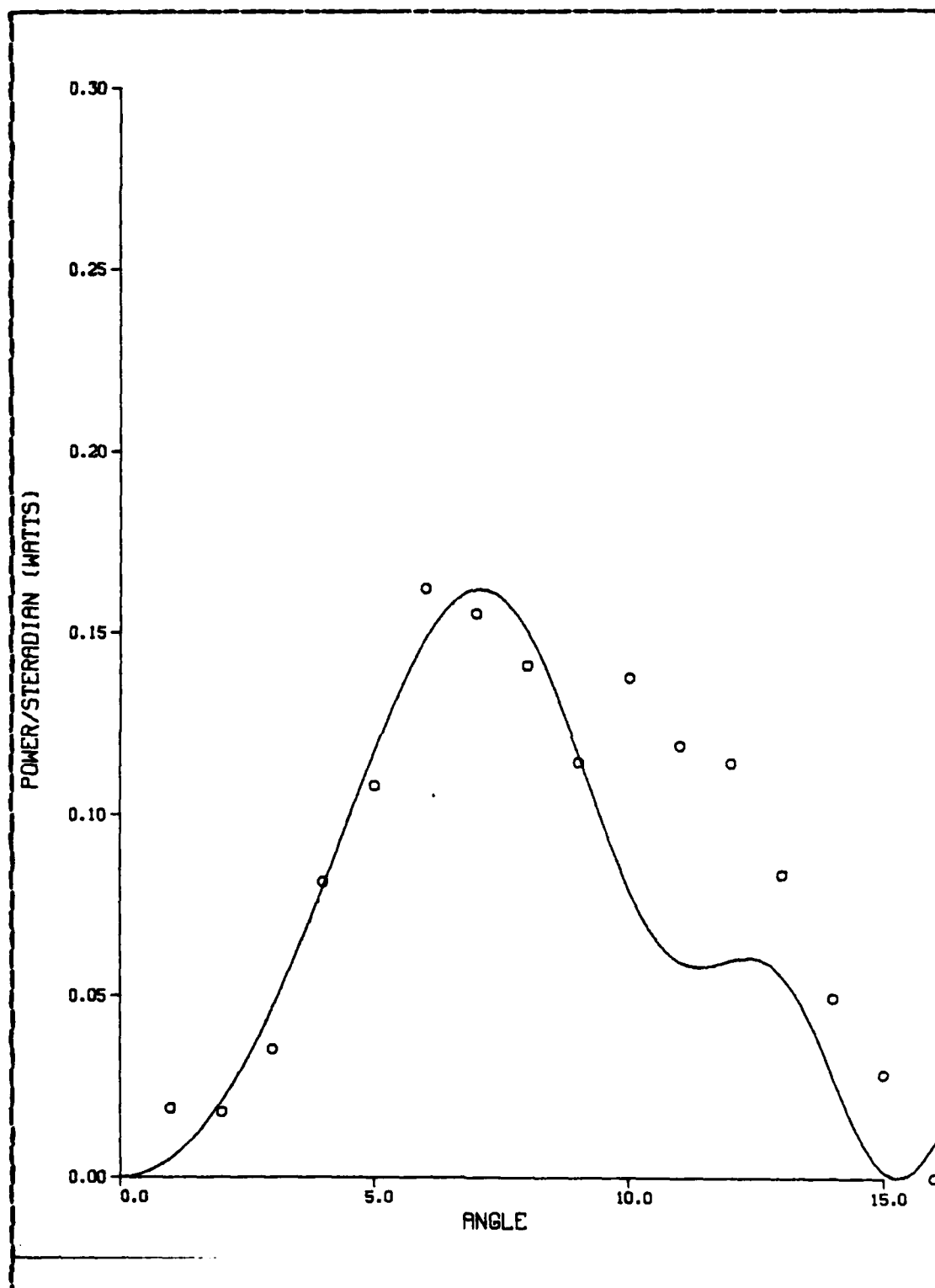


Figure 3.5 Harmonics= 3 + 6 : L=1.0 m : Filter = 3rd.

C. CONCLUSIONS

The results presented here demonstrate initial confirmation of the theory. Although it is difficult to improve the geometry of the experiment, definite improvements can be made in the measurement of the microwave radiation. Instead of using waveguide filters and a crystal detector (the use of which leads to measurement ambiguities for harmonics greater than the fourth), a tunable YIG filter coupled to a spectrum analyzer of appropriate sensitivity should be used. This will enable the observer to isolate harmonics for measurement without ambiguity, as well as allowing the measurement of absolute (vice relative) power.

APPENDIX A

FORTRAN PROGRAM FOR CALCULATING CERENKOV RADIATION CURVES

This is an interactive program which calculates and plots Cerenkov radiation curves for the case of a finite path length. Up to five different harmonics of the electron bunch frequency and five different lengths of emission path may be selected for presentation. The program also allows for adjustment of all basic parameters and constants of the Cerenkov power equation. A different curve will be plotted for each distinct combination of path length and harmonic.

```

C THIS PROGRAM CALCULATES AND PLOTS CERENKOV RADIATION CURVES. UP TO
C FIVE HARMONICS AND FIVE LENGTHS OF EMISSION REGION MAY BE CHOSEN.
C A DIFFERENT CURVE WILL BE PLOTTED FOR EACH DISTINCT COMBINATION OF
C LENGTH AND HARMONIC.
      REAL N, MU, KAY, MU, NUO, IF,B,C,GAMMA,BETA,V,COSTC,
      * C1,UF,CO,N,MU,NUO,Q,E,MO,E
      DIMENSION W(1000), THETA(1000), HARM(5), CELL (5)
C
C INITIALIZE CONSTANTS
      DATA ICC/CO, //IA/N, //IMU/MO, //INUO/NUO, //,IB/B, //,IY/Y, //,IND/N, /
      * IQ/Q, //IE/E
      NPCINT = 101
      THETAF = 20.0
      PI = 3.14159265359
      DGTIRC = 0.0174532525199
      RDTCDG = 57.29577951308
C
C *** INITIALIZE PROGRAM CONSTANTS
      CO = 2.997925E08
      N = 1.000268E00
      MU = 1.256E-06
      NUC = 2.85E09
      Q = 1.94E-12
      E = 1.6E-11
      MO = 5.10953E-31
      B = .0024E00
C
C *** ARE PROGRAM CONSTANTS OK?
      WRITE(6,90C) CO,N,MU,NUO,Q,E,MO,B
      READ(5,501) IANS
      IF (IANS.EQ.INC) GC TO 40
C *** NO, PROGRAM CONSTANTS NEED TO BE CHANGED
      WRITE(6,902),
      READ(5,503) IANS
C
      IF (IANS.NE.IC0) GO TO 11
      WRITE(6,504) IANS
      READ(5,505) CO
      GC TC 10
C
C 11
      IF (IANS.NE.IN) GO TO 12
      WRITE(6,904) IANS
      READ(5,506) N
      GC TC 10
C
C 12
      IF (IANS.NE.IMU) GO TO 13
      WRITE(6,904) IANS

```

CEROC490
CEROC500
CEROC510
CEROC520
CEROC530
CEROC540
CEROC550
CEROC560
CEROC570
CEROC580
CEROC590
CEROC600
CEROC610
CEROC620
CEROC630
CEROC640
CEROC650
CEROC660
CEROC670
CEROC680
CEROC690
CEROC700
CEROC710
CEROC720
CEROC730
CEROC740
CEROC750
CEROC760
CEROC770
CEROC780
CEROC790
CEROC800
CEROC810
CEROC820
CEROC830
CEROC840
CEROC850
CEROC860
CEROC870
CEROC880
CEROC890
CEROC900
CEROC910
CEROC920
CEROC930
CEROC940
CEROC950

```

C13      READ (5,*) MU
          GO TO 10
          IF(IANS.NE.INUO) GO TO 14
          WRITE (6,904) IANS
          READ (5,*) NUO
          GO TO 10

C14      IF(IANS.NE.IQ) GO TO 15
          WRITE (6,904) IANS
          READ (5,*) C
          GO TO 10

C15      IF(IANS.NE.IE) GO TO 16
          WRITE (6,904) IANS
          READ (5,*) E
          GO TO 10

C16      IF(IANS.NE.IMO) GO TO 17
          WRITE (6,904) IANS
          READ (5,*) MO
          GO TO 10

C17      IF(IANS.NE.IB) GO TO 18
          WRITE (6,904) IANS
          READ (5,*) B
          GO TO 10

C18      *** ERRCR
          WRITE (6,910)
          GO TO 10

C40      WRITE (6,505)
          READ (5,*) HARM(1),HARM(2),HARM(3),HARM(4),HARM(5)
          WRITE (6,506)
          READ (5,*) CELL(1),CELL(2),CELL(3),CELL(4),CELL(5)

          CALL TEK618
          CALL PTEKAL
          CALL PRTPLOT(72,6)
          CALL VRSTEC(0,0,0)
          CALL CCMPRS

          CALL NCERDR
          CALL PAGE(8.5,11.0)

          C THE LOCATION OF THE ORIGIN:
            CALL PHYSOR(1.0,1.0)

```



```

C 80      WRITE(50,*) W(1),THETA(1),F,IF
C          CONTINUE
C          CALL CURVE FOR EACH CURVE DESIRED (Q IN LAST PARAMETER
C          INDICATES DO NOT DISPLAY DATA POINTS, 1 MEANS DISPLAY
C          EVERY DATA POINT)
C          CALL CLFVE (THETA,W,NPOINT,0)
C          CALL CLFVE (X,Y,N,0)
C          CALL CLFVE (X,Y,N,0)
C 75      CONTINUE
C 70      CONTINUE
C          CALL ENDPL(0)
C          ** USER WANT ANOTHER RUN?
C          WRITE(6,508)
C          REAL(5,901) IANS
C          IF (IANS.EQ.1) GO TO 10
C          CONTINUE
C          STGP
C 90
C 900      FORMAT(/,' PROGRAM CONSTANTS CURRENTLY HAVE VALUES AS FOLLOWS:','/
C          * 5X,'CC' = SPEED OF LIGHT IN VACUUM = 2.9979E14.7, //
C          * 5X,'N' = AIR REFRACTIVE INDEX = 1.00027, //
C          * 5X,'ML' = PERMEABILITY OF AIR = 1.2566E-06, //
C          * 5X,'NLO' = BUNCH FREQUENCY = 1.0E14.7, //
C          * 5X,'C' = ELECTRON CHARGE = 1.6021E-19, //
C          * 5X,'E' = ELECTRON ENERGY = 1.6021E-19, //
C          * 5X,'MC' = ELECTRON REST MASS = 9.1091E-31, //
C          * 5X,'B' = ELECTRON SIZE PARAMETER = 1.0E14.7, //
C          * 5X,'DO YOU WANT TO CHANGE ANY OF THESE VALUES? (Y OR N)')
C          FORMAT(A1)
C          FORMAT(/,' ENTER CCNSTANT TO BE CHANGED:')
C          FORMAT(A4)
C          FORMAT(/,' ENTER NEW VALUE FOR 'A4,':')
C          FORMAT(/,' ENTER VALUES FOR HARM (HARMONIC OF BUNCH FREQUENCY):')
C          FORMAT(/,' ENTER VALUES FOR CELL (LENGTH OF EMISSION REGION):')
C          FORMAT(/,' ENTER ANOTHER RUN? (ENTER Y OR N)')
C          FORMAT(/,' THE VARIABLE SELECTED IS NOT IN THE LIST - TRY AGAIN')
C          END
C 901
C 902
C 903
C 904
C 905
C 906
C 908
C 910
C 9011450
C 9011460
C 9011470
C 9011480
C 9011490
C 9011500
C 9011510
C 9011520
C 9011530
C 9011540
C 9011550
C 9011560
C 9011570
C 9011580
C 9011590
C 9011600
C 9011610
C 9011620
C 9011630
C 9011640
C 9011650
C 9011660
C 9011670
C 9011680
C 9011690
C 9011700
C 9011710
C 9011720
C 9011730
C 9011740
C 9011750
C 9011760
C 9011770
C 9011780
C 9011790
C 9011800
C 9011810
C 9011820
C 9011830
C 9011840
C 9011850
C 9011860
C 9011870
C 9011880
C 9011890
C 9011900

```

APPENDIX B
FORTRAN PROGRAM - CERENKOV CURVES WITH DATA POINTS

This is an interactive program which calculates and plots several Cerenkov radiation curves as well as a single set of experimentally observed data points. Up to five different harmonics of the bunch frequency and five different lengths of the emission path may be chosen for presentation. A different curve will be plotted for each distinct combination of path length and harmonic. The program also allows adjustment of all basic parameters and constants of the Cerenkov power equation. The program then prompts for 20 data measurements of power (one per degree) which will be superimposed over the curves.

```

C C C C C
THIS PROGRAM CALCULATES AND PLOTS CERENKOV RADIATION CURVES FOR
UP TO FIVE DIFFERENT HARMONICS AND FIVE DIFFERENT LENGTHS OF
EMISSION REGION. A DIFFERENT CURVE WILL BE CALCULATED FOR EACH
DISTINCT COMBINATION OF LENGTH AND HARMONIC. THE PROGRAM THEN ASKS
FOR 20 DATA POINTS (ONE PER DEGREE) TO BE SUPERIMPOSED OVER THE
CURVES.
C C C C C
      REAL N, MU, KAY, MO, NUO, IF, B, C, GAMMA, BETA, V, COSTC,
      C1, U, F, CO, N, MU, NUG, Q, E, MO, E
* DIMENSION W(1000), THETA(1000), HARM(5), CELL (5), THETAP(20),
* PCWER(20)
C C
      INITIALIZE CONSTANTS
      DATA ICC/CO, IIN/IN, IIE/IE, IMU/MU, INUC/NUO, IB/IB, IY/Y, INO/NO,
* NPCINT = 101
      THETAP = 20
      PI = 3.14159265359
      DGTICRD = 0
      RDTCOG = 57.29577551308
C C
      *** INITIALIZE PROGRAM CONSTANTS
      CO = 2.997925E08
      N = 1.0000268E00
      MU = 1.256E-06
      NUO = 2.85E09
      Q = 1.94E-12
      E = 1.6E-11
      MO = 5.10953E-31
      B = .0024E00
C C
      *** ARE PROGRAM CONSTANTS OK?
      WRITE(6,900) CO, N, MU, NUO, Q, E, MO, B
      REAL(5,901) IANS
      IF (IANS.EQ.INC) GC TO 40
      *** NO PROGRAM CONSTANTS NEED TO BE CHANGED
      WRITE(6,902)
      REAL(5,903) IANS
C C
      IF (IANS.NE.IC0) GO TO 11
      WRITE(6,904) IANS
      READ(5,905) CO
      GC TC 10
C 11
      IF (IANS.NE.IN) GO TO 12
      WRITE(6,904) IANS
      READ(5,905) N
      GC TC 10
C 10
C C C C C
CER00C10
CER00C20
CER00C30
CER00C40
CER00C50
CER00C60
CER00C70
CER00C80
CER00C90
CER00C100
CER00C110
CER00C120
CER00C130
CER00C140
CER00C150
CER00C160
CER00C170
CER00C180
CER00C190
CER00C200
CER00C210
CER00C220
CER00C230
CER00C240
CER00C250
CER00C260
CER00C270
CER00C280
CER00C290
CER00C300
CER00C310
CER00C320
CER00C330
CER00C340
CER00C350
CER00C360
CER00C370
CER00C380
CER00C390
CER00C400
CER00C410
CER00C420
CER00C430
CER00C440
CER00C450
CER00C460
CER00C470
CER00C480

```

CEROC490
 CEROC500
 CEROC510
 CEROC520
 CEROC530
 CEROC540
 CEROC550
 CEROC560
 CEROC570
 CEROC580
 CEROC590
 CEROC600
 CEROC610
 CEROC620
 CEROC630
 CEROC640
 CEROC650
 CEROC660
 CEROC670
 CEROC680
 CEROC690
 CEROC700
 CEROC710
 CEROC720
 CEROC730
 CEROC740
 CEROC750
 CEROC760
 CEROC770
 CEROC780
 CEROC790
 CEROC800
 CEROC810
 CEROC820
 CEROC830
 CEROC840
 CEROC850
 CEROC860
 CEROC870
 CEROC880
 CEROC890
 CEROC900
 CEROC910
 CEROC920
 CEROC930
 CEROC940
 CEROC950
 CEROC960

```

C 12      IF(IANS.NE.IMU) GO TO 13
           WRITE(6,904) IANS
           READ(5,*) MU
           GC TC 10

C 13      IF(IANS.NE.INUO) GO TO 14
           WRITE(6,904) IANS
           READ(5,*) NUO
           GC TC 10

C 14      IF(IANS.NE.IQ) GO TO 15
           WRITE(6,904) IANS
           READ(5,*) Q
           GC TC 10

C 15      IF(IANS.NE.IE) GO TO 16
           WRITE(6,904) IANS
           READ(5,*) E
           GC TC 10

C 16      IF(IANS.NE.IMO) GO TO 17
           WRITE(6,904) IANS
           READ(5,*) MO
           GC TC 10

C 17      IF(IANS.NE.IB) GO TO 18
           WRITE(6,904) IANS
           READ(5,*) B
           GC TC 10

C 18      *** ERROR
           WRITE(6,910)
           GC TO 10

C 40      WRITE(6,905)
           READ(5,*) HARM(1),HARM(2),HARM(3),HARM(4),HARM(5)
           WRITE(6,906)
           READ(5,*) CELL(1),CELL(2),CELL(3),CELL(4),CELL(5)

C          WRITE(6,907)
           DO 41 I = 1,20
             READ(5,*) POWER(I)
             CONTINUE

C 41      DO 42 I = 1,20
             IF(TAP(I) = I
             CONTINUE

C 42      CONTINUE
  
```

```

C      CALL TEK618
C      CALL PTEKAL
C      CALL PRTPLOT(72,6)
C      CALL VRSTEC(0,0,0)
C      CALL CCFPRS
C
C      CALL NCERDR
C      CALL PAGE(8.5,11.0)
C
C      THE LOCATION OF THE ORIGIN:
C      CALL PHYSOR(1.0,1.0)
C
C      THE AREA IN INCHES BY INCHES:
C      CALL AREA2D(7.0,10.0)
C
C      WHATEVER LABELS DESIRED ON X AND Y AXIS:
C      CALL XNAME('ANGLE $',100)
C      CALL YXANG(0)
C      CALL YNAME('POWER/STERADIAN (WATTS)' ,100)
C
C      WHATEVER HEADING DESIRED FOR GRAPH:
C      CALL HEADIN('THIS IS A HEADING$',100,1.2,2)
C      CALL HEADIN('HEADING ON NEXT LINE$',100,1.2,2)
C
C      RANGE AND INCREMENTS CF X AND RANGE AND INCREMENTS OF Y
C      CALL GRAF(0.0, 5.0,15.0, 0.0, .01,0.15)
C
C      NEED SPLINE FOR SMOOTH FIT (OTHERWISE GET LINEAR FIT)
C      CALL SPLINE
C      DO 70 J=1,5
C      IF (HARM(J).EQ.0) GC TO 70
C          DO 75 K=1,5
C          IF (CELL(K).EQ.0) GO TO 70
C          *** BEGIN CALCULATIONS
C          C = CO / N
C          GAMMA = E / (MO*CO*CO)
C          BETA = (1.0 - 1.0 / (GAMMA*GAMMA)) ** 0.5
C          V = BETA * CO
C          CCSTC = C / V
C          C1 = MU*C*NUC*NUO*Q*Q / (8.0*PI*PI)
C          KAY = 2.0*PI*HARM(J)*NUO / C
C          WRITE(50,*) KAY,COSTC,HARM(J), CELL(K)
C

```

```
C C *** CALCULATE FUNCTIONAL VALUES
C RACF = THETA F * DGTORD
C XPOINT = FLOAT(NPCINT-1)
C DC 80 I=1,NPCINT
C   RATIO = FLCAT(I-1) / XPOINT
C   ANGLE = RATIO * RADF
C   THETA(I) = RATIO * THETAF
C   F = 1/(EXP(0.25 * B*KAY*COS(ANGLE) + B*KAY*COS(ANGLE)))/2
C   U = (KAY * CELL(K) * (COSTC-COS(ANGLE)))**2
C   IF = SIN(U) / U
C   W(I) = C1 * (F*KAY*CELL(K)*SIN(ANGLE)*IF)**2
C WRITE(50,*) W(I),THETA(I),F,IF
C CONTINUE
C CALL CURVE FOR EACH CURVE DESIRED (0 IN LAST PARAMETER
C INDICATES CG NOT DISPLAY DATA POINTS, 1 MEANS DISPLAY
C EVERY DATA POINT)
C CALL CLFV (THETA,W,NPOINT,0)
C CALL CLFVE (X,Y,N,0)
C CALL CLFVE (X,VY,N,0)
C 75 CONTINUE
C 70 CONTINUE
C CALL CURVE (THETAP,POWER,20,-1)
C CALL ENCLP(C)
C ** USER WANT ANOTHER RUN?
C   WRITE(6,508)
C   REAC(51901) IANS
C   IF(IANS.EQ.IY) GC TC 10
C CALL DCNEPL
C CONTINUE
C STCP
C 90
C 900 FORMAT(/,' PROGRAM CONSTANTS CURRENTLY HAVE VALUES AS FOLLOWS:',/
C ,5X,'CC' = SPEED OF LIGHT IN VACUUM
C ,5X,'NL' = AIR REFRACTIVE INDEX
C ,5X,'ML' = PERMEABILITY CF AIR
C ,5X,'AL0' = BUNCH FREQUENCY
C ,5X,'CE' = ELECTRON CHARGE
C ,5X,'EC' = ELECTRON REST MASS
C ,5X,'NC'
```

1234567890
0000000000
9999999999

APPENDIX C

FORTRAN PROGRAM - SUM OF CERENKOV CURVES WITH DATA POINTS

This is an interactive program which calculates and plots a single Cerenkov radiation curve and superimposes a single set of data points over the curve. The single Cerenkov curve will represent a sum of curves. The sum will be composed of each distinct combination of harmonic and path length chosen. Up to five different lengths of emission path and five different harmonics of the bunch frequency may be chosen. The program also allows adjustment of all basic parameters and constants of the Cerenkov power equation. The program will prompt for 20 data measurements of power (one for each degree of angle).

```

C THIS PROGRAM CALCULATES AND PLOTS A SUM OF CERENKOV RADIATION
C CURVES. UP TO FIVE HARMONICS AND FIVE LENGTHS OF EMISSION REGION
C MAY BE CHOSEN; THE PROGRAM WILL INCLUDE A DIFFERENT CURVE IN THE SUM
C FOR EACH DISTINCT COMBINATION OF LENGTH AND HARMONIC. THE PROGRAM
C THEN ASKS FOR 20 DATA POINTS (ONE PER DEGREE) TO BE SUPERIMPOSED
C OVER THE CURVE.
C
C REAL N, MU, KAY, MO, NUO, IF, B, C, GAMMA, BETA, V, COSTC,
C C1, U, F, CO, N, MU, NUO, Q, E, MO, E
C * DIMENSION W(1000), THETA(1000), HARM(5), CELL(5), THETAP(20),
C * PCWER(20), SUM(1000)
C
C INITIALIZE CONSTANTS
C DATA ICC/CO, IE/IE, IN/IN, IMU/MO, INUQ/NUO, IB/IE, IY/Y, INO/N, /
C *
C NPICINT = 101.0
C THETAP = 20.55265359
C PI = 3.14159265359
C DGTCDG = 0.0174532525199
C ROTCDG = 57.29577551308
C
C *** INITIALIZE PROGRAM CONSTANTS
C CO = 2.997925E08
C N = 1.000268E00
C MU = 1.254E-06
C NUC = 2.855E09
C Q = 1.94E-12
C E = 1.6E-11
C MO = 5.10553E-31
C B = .0024E00
C
C ARE PROGRAM CONSTANTS OK?
C WRITE(6,900) CO, N, MU, NUO, Q, E, MO, B
C READ(5,901) IANS
C IF (IANS.EQ.INC) GC TO 40
C *** NO, PROGRAM CONSTANTS NEED TO BE CHANGED
C WRITE(6,902)
C READ(5,903) IANS
C
C IF (IANS.NE.IC0) GO TO 11
C WRITE(6,904) IANS
C READ(5,905) CO
C GC TC 10
C
C IF (IANS.NE.IN) GO TO 12
C WRITE(6,904) IANS
C READ(5,905) N
C GC TC 10
C
SUM00010
SUM00020
SUM00030
SUM00040
SUM00050
SUM00060
SUM00070
SUM00080
SUM00090
SUM00100
SUM00110
SUM00120
SUM00130
SUM00140
SUM00150
SUM00160
SUM00170
SUM00180
SUM00190
SUM00200
SUM00210
SUM00220
SUM00230
SUM00240
SUM00250
SUM00260
SUM00270
SUM00280
SUM00290
SUM00300
SUM00310
SUM00320
SUM00330
SUM00340
SUM00350
SUM00360
SUM00370
SUM00380
SUM00390
SUM00400
SUM00410
SUM00420
SUM00430
SUM00440
SUM00450
SUM00460
SUM00470
SUM00480

```

SUM0C490
SUM0C500
SUM0C510
SUM0C520
SUM0C530
SUM0C540
SUM0C550
SUM0C560
SUM0C570
SUM0C580
SUM0C590
SUM0C600
SUM0C610
SUM0C620
SUM0C630
SUM0C640
SUM0C650
SUM0C660
SUM0C670
SUM0C680
SUM0C690
SUM0C700
SUM0C710
SUM0C720
SUM0C730
SUM0C740
SUM0C750
SUM0C760
SUM0C770
SUM0C780
SUM0C790
SUM0C800
SUM0C810
SUM0C820
SUM0C830
SUM0C840
SUM0C850
SUM0C860
SUM0C870
SUM0C880
SUM0C890
SUM0C900
SUM0C910
SUM0C920
SUM0C930
SUM0C940
SUM0C950

```

C 12 IF(IANS,NE,IMU) GO TO 13
      WRITE(6,904) IANS
      READ(5,*) MU
      GC TC 10

C 13 IF(IANS,NE,INUC) GO TO 14
      WRITE(6,904) IANS
      READ(5,*) NUO
      GO TC 10

C 14 IF(IANS,NE,IQ) GO TC 15
      WRITE(6,904) IANS
      READ(5,*) C
      GC TC 10

C 15 IF(IANS,NE,IE) GO TC 16
      WRITE(6,904) IANS
      READ(5,*) E
      GO TC 10

C 16 IF(IANS,NE,IMO) GO TO 17
      WRITE(6,904) IANS
      READ(5,*) MO
      GC TC 10

C 17 IF(IANS,NE,IB) GO TO 18
      WRITE(6,904) IANS
      READ(5,*) B
      GC TC 10

C 18 *** ERROR
      WRITE(6,910)
      GO TO 10

C 40 WRITE(6,905)
      READ(5,*) HARM(1), HARM(2), HARM(3), HARM(4), HARM(5)
      WRITE(6,906)
      READ(5,*) CELL(1), CELL(2), CELL(3), CELL(4), CELL(5)

C      WRITE(6,907)
      DO 41 I = 1,20
      CONTINUE
      DO 42 I = 1,20
      IFETAP(I) = 1
      CONTINUE

```



```

C      C1 = MU*C*NUO*NUO*Q*C / (8.0*PI*PI)
C      KAY = 2.0*PI*HARM(J)*NUO / C
C      WRITE(50,*) KAY,COSTC,HARM(J), CELL(K)

*** CALCULATE FUNCTIONAL VALUES
RADF = THETA*F*DGTDORD
XFCINT = FLOAT(NPOINT-1)
CC 80 I=1,NPCINT
    RATIO = FLQAT(I-1) / XPOINT
    ANGLE = RATIO*RADF
    THETA(I) = RATIO*THETA
    F = 1/(EXP(0.25*B*KAY*COS(ANGLE)*B*KAY*COS(ANGLE)))/2
    IF = SIN(U) / (F*KAY*CELL(K)*SIN(ANGLE)*IF)**2
    W(I) = C1*(F*KAY*CELL(K)*SIN(ANGLE)*IF)**2
    SUM(I) = W(I) + SUM(I)
    WRITE(50,*) SUM(I),THETA(I)
    WRITE(50,*) W(I),THETA(I),F,IF
    CONTINUE

CALL CURVE FOR EACH CURVE DESIRED (O IN LAST PARAMETER
INDICATES CC NOT DISPLAY DATA POINTS, I MEANS CISPPLAY
EVERY DATA POINT)
CALL CURVE (THETA,W,NPOINT,O)
CALL CURVE (X,Y,N,O)
CALL CURVE (X,YY,N,O)

CONTINUE
CONTINUE
CONTINUE
CALL CURVE (THETA,SUM,NPOINT,O)
CALL CURVE (THETA,POWER,20,-1)
CALL ENCL(0)

** USER WANT ANOTHER RUN?
WRITE(6,508)
REAL(5,901) IANS
IF (IANS.EQ.1Y) GO TO 10
CALL DCNEPL
CONTINUE
STOP

90
C 900 FORMAT(/,' PROGRAM CONSTANTS CURRENTLY HAVE VALUES AS FOLLOWS: ',/
SUM01450
SUM01460
SUM01470
SUM01480
SUM01490
SUM01500
SUM01510
SUM01520
SUM01530
SUM01540
SUM01550
SUM01560
SUM01570
SUM01580
SUM01590
SUM01600
SUM01610
SUM01620
SUM01630
SUM01640
SUM01650
SUM01660
SUM01670
SUM01680
SUM01690
SUM01700
SUM01710
SUM01720
SUM01730
SUM01740
SUM01750
SUM01760
SUM01770
SUM01780
SUM01790
SUM01800
SUM01810
SUM01820
SUM01830
SUM01840
SUM01850
SUM01860
SUM01870
SUM01880
SUM01890
SUM01900
SUM01910
SUM01920

```

[illegible]

APPENDIX D

EXPERIMENTAL APPARATUS

This appendix contains photographs of the experimental apparatus used in this experiment. Figure D.1 shows the end station of the LINAC. At the right is the LINAC beam aperture, with the reflecting aluminum mirror at the left. The detector assembly, mounted at the end of the pivot arm, is shown in the foreground of the photograph. Also shown, located along the beam path between the aperture and the mirror, is a small portable laser used to align the mirror.

Figure D.2 shows the waveguide filter with the fin-line insert for one of the harmonics, along with the detector and horn. Figure D.3 shows the detector apparatus assembled.



Figure D.1 LINAC End-Station.

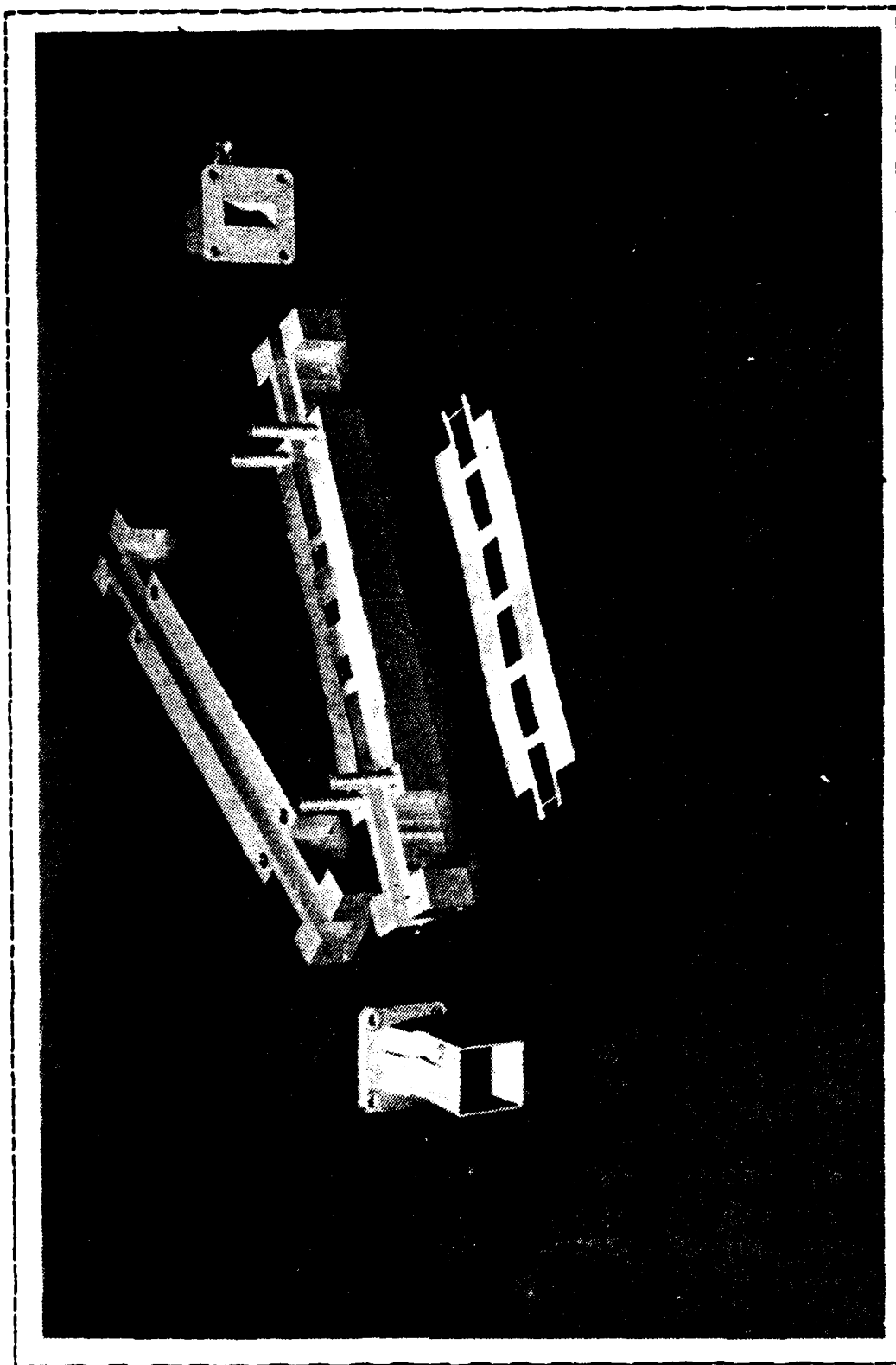


Figure D.2 Detection Apparatus Components.

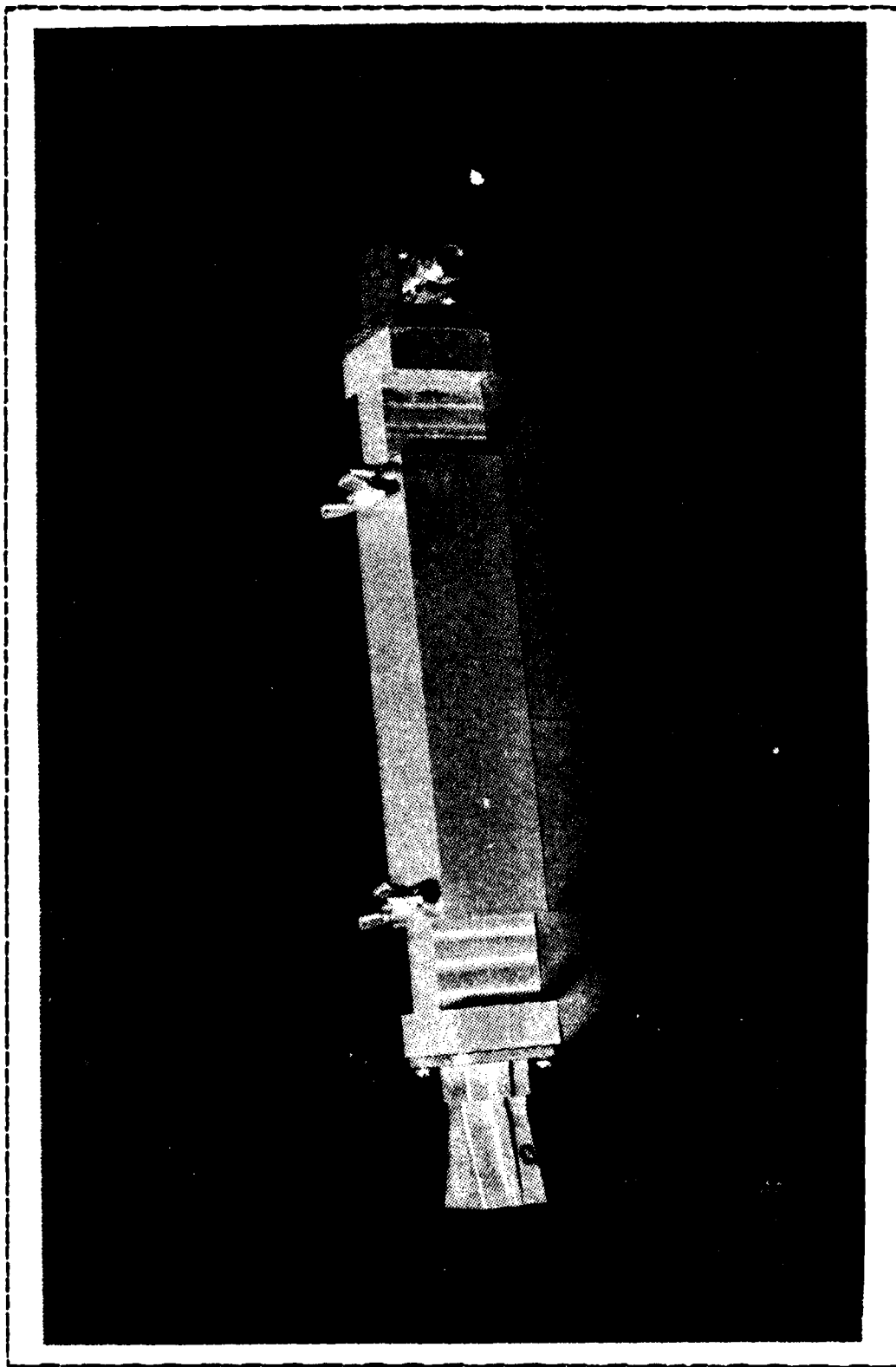


Figure D.3 Assembled Detection Apparatus.

APPENDIX E
TABULAR DATA FOR FIGURES

TABLE III
Tabular Data for Figure 3.1

Degree	Channel	Normalized Value
1	101	.0082
2	96	.0078
3	188	.0153
4	434	.0352
5	575	.0467
6	864	.0701
7	828	.0672
8	752	.0610
9	610	.0495
10	734	.0596
11	635	.0515
12	609	.0494
13	446	.0362
14	265	.0215
15	152	.0123

-Channel values were read from the Pulse Height Analyzer

-Normalizing factor was $8.1134\text{E-}05$

-Beam current = $4.0\text{E-}08$ Amps

TABLE IV
Tabular Data for Figure 3.2

Degree	Channel	Normalized Value
1	219	.0244
2	114	.0127
3	198	.0221
4	284	.0317
5	556	.0620
6	694	.0774
7	772	.0861
8	786	.0877
9	572	.0638
10	393	.0438
11	304	.0339
12	193	.0215
13	190	.0212
14	64	.0071
15	0	.0000

- Channel values were read from Pulse Height Analyzer
- Normalizing factor was 1.1158E-04
- Beam current = 4.0E-08 Amps

TABLE V
Tabular Data for Figure 3.3

Degree	Channel	Normalized Value
1	117	.0837
2	0	.0000
3	75	.0537
4	207	.1481
5	431	.3083
6	565	.4042
7	623	.4457
8	590	.4221
9	556	.3978
10	442	.3162
11	344	.2461
12	262	.1874
13	210	.1502
14	111	.0794
15	109	.0780

-Channel values were read from Pulse Height Analyzer

-Normalizing Factor was 3.9502E-04

-Beam current = 4.0E-08 Amps

TABLE VI
Tabular Data for Figure 3.4

Degree	Channel	Normalized Value
1	117	.0290
2	0	.0000
3	75	.0186
4	207	.0513
5	431	.1069
6	565	.1401
7	623	.1545
8	590	.1463
9	556	.1379
10	442	.1096
11	344	.0853
12	262	.0650
13	210	.0521
14	111	.0275
15	109	.0270

- Channel Values were read from the Pulse Height Analyzer
- Normalizing factor was $2.48E-04$
- Beam current = $4.0E-08$ Amps

TABLE VII
Tabular Data for Figure 3.5

Degree	Channel	Normalized Value
1	101	.0190
2	96	.0180
3	188	.0353
4	434	.0815
5	575	.1080
6	864	.1623
7	828	.1555
8	752	.1413
9	610	.1146
10	734	.1379
11	635	.1193
12	609	.1144
13	446	.0838
14	265	.0498
15	152	.0286

- Channel values were read from the Pulse Height Analyzer
- Normalizing factor was $1.878\text{E}-04$
- Beam current = $4.0\text{E}-08$ Amps

LIST OF REFERENCES

1. Buskirk, P. R. and Neighbours, J. R., "Cerenkov Radiation from Periodic Electron Bunches," Physical Review, v. 28, pp. 1531-1538, September 1983.
2. Naval Postgraduate School, Report Number NPS-61-83-003, Cerenkov Radiation from Bunched Electron Beams, by P. R. Buskirk and J. R. Neighbours, October 1982.
3. Naval Postgraduate School, Report Number NPS-61-83-010, Diffraction Effects in Cerenkov Radiation, by J. R. Neighbours and P. R. Buskirk, June 1983.
4. Saglam, Ahmet, Cerenkov Radiation, Master's Thesis, Naval Postgraduate School, Monterey, 1982.
5. Alexander, K. B., and Hamel, S. R., Design and Analysis of a Generalized Class of Fin-Line Filters, Master's Thesis, Naval Postgraduate School, Monterey, 1983.
6. Collin, R. E., Foundations for Microwave Engineering, Mc-Graw Hill, 1966.

INITIAL DISTRIBUTION LIST

	No. Copies
1. Defense Technical Information Center Cameron Station Alexandria, Virginia 22314	2
2. Superintendent Attn: Library, Code 0142 Naval Postgraduate School Monterey, California 93943	2
3. Physics Library, Code 61 Department of Physics Naval Postgraduate School Monterey, California 93943	2
4. Professor F. R. Buskirk, Code 51Bs Department of Physics Naval Postgraduate School Monterey, California 93943	10
5. Professor J. R. Neighbours, Code 61Nb Department of Physics Naval Postgraduate School Monterey, California 93943	2
6. Lieutenant Lawrence A. Newton Naval Ship Weapons Systems Engineering Station Port Hueneme, California 93043	2
7. Dr. Charles M. Huddleston, Code R401 Naval Surface Weapons Center Silver Spring, Missouri 20810	2
8. Captain Robert Topping PMS 405 Naval Sea Systems Command Washington, D.C. 20362	2

END

FILMED

ADTIC